EE 213, Microscopic Nanocharacterization of Materials
Lecture 8.
other micro-characterization using charged particle beams

Class website: https://ee213-winter16-01.courses.soe.ucsc.edu

Mike Isaacson, Baskin 237
Email: msi@soe.ucsc.edu
Tele: 831-459-3190
Admin. Asst. Rachel Cordero: rcordero@soe.ucsc.edu, 831-459-2921

Crystal Spectrometer geometry

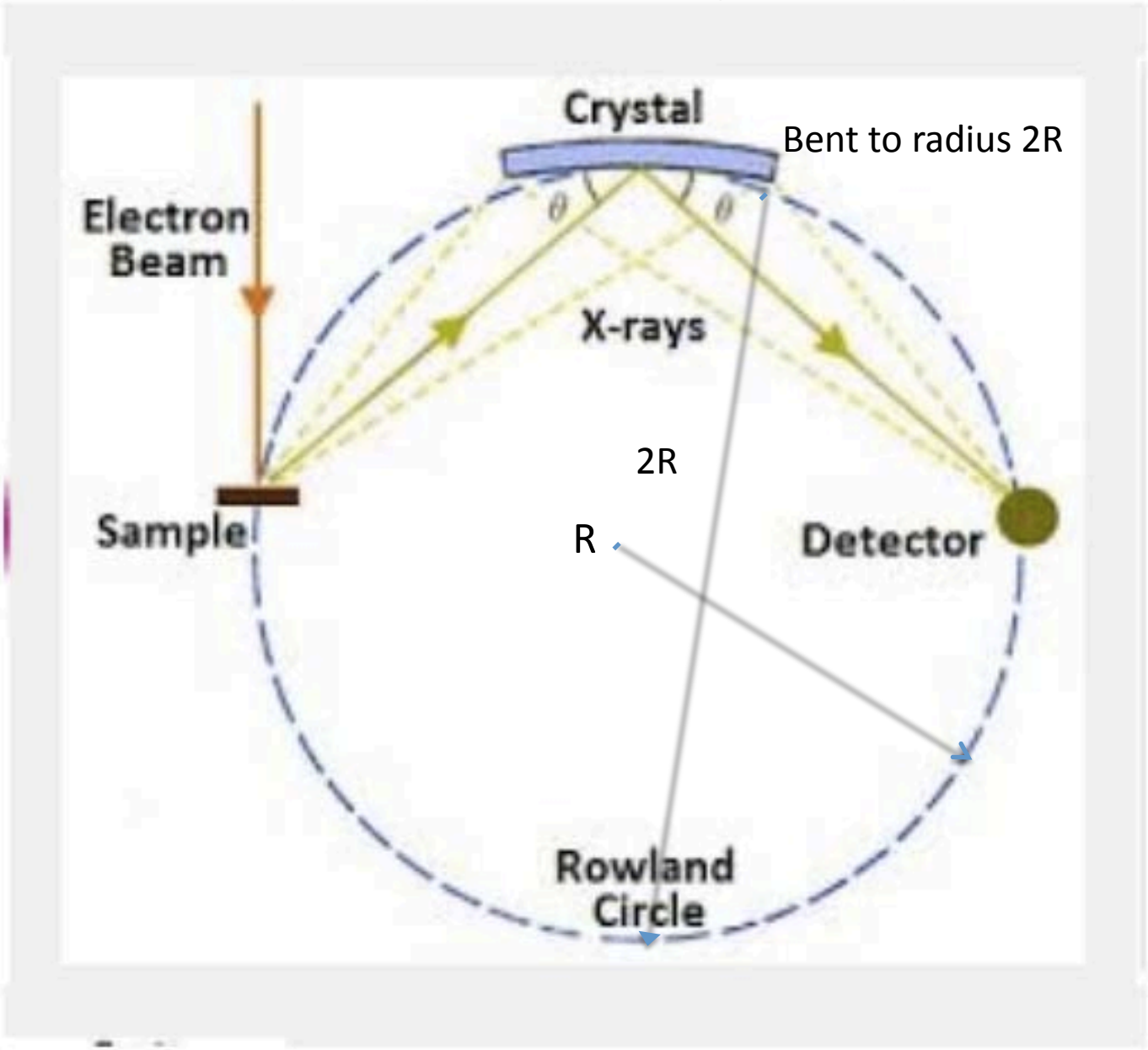

Henry Augustus Rowland

Henry Augustus Rowland (1848-1901)

Born	November 27, 1848 Honesdale, Pennsylvania, U.S.
Died	April 16, 1901 (aged 52) Baltimore, Maryland, U.S.
Nationality	American
Fields	Physicist
Institutions	University of Wooster Rensselaer Polytechnic Institute Johns Hopkins University

1st chair of physics at Johns Hopkins University

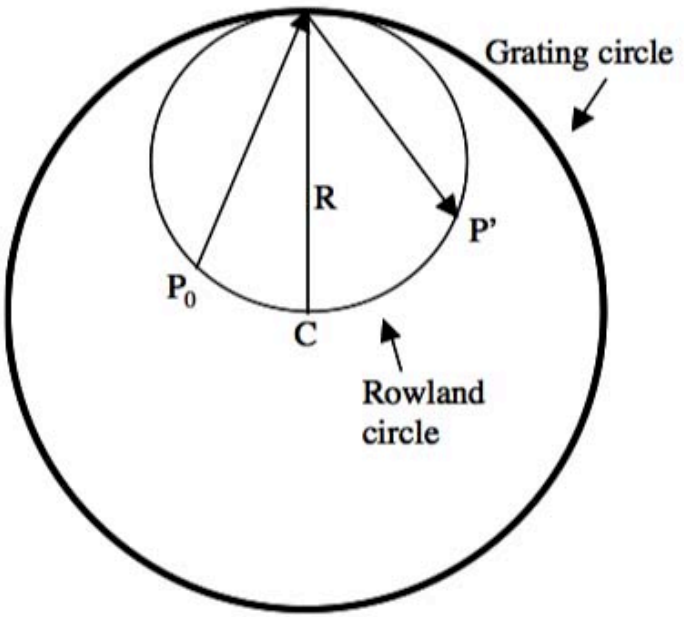

Figure A.2: Rowland circle geometry

Rowland Circle Arrangement

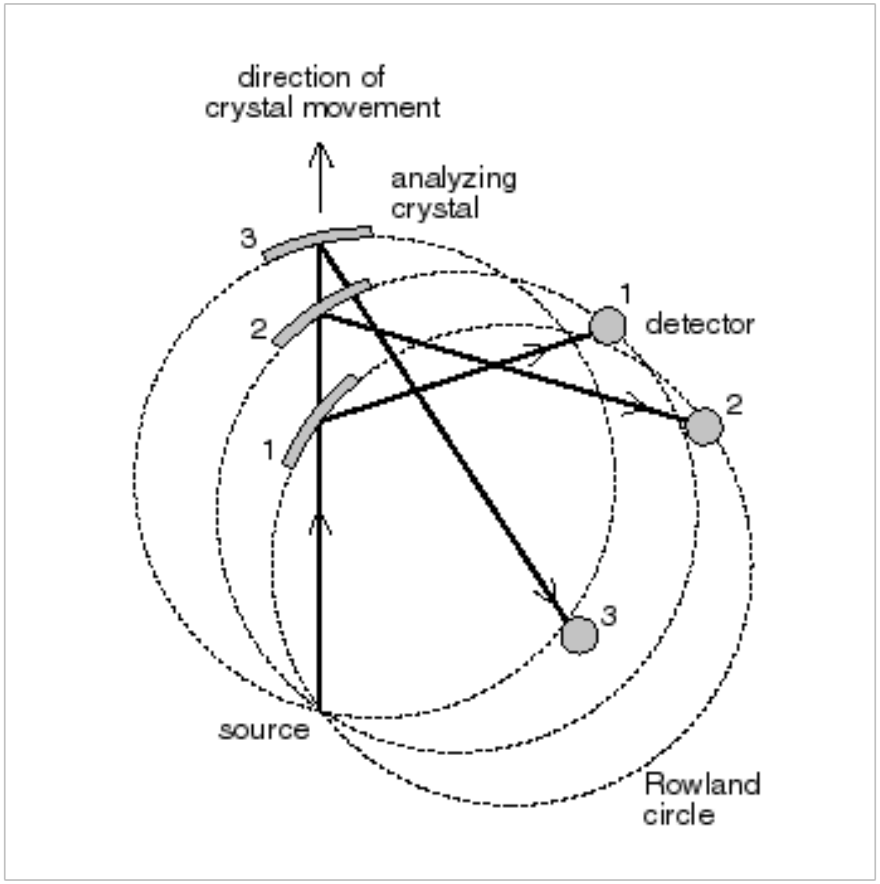

Generic EMPA/SEM WDS

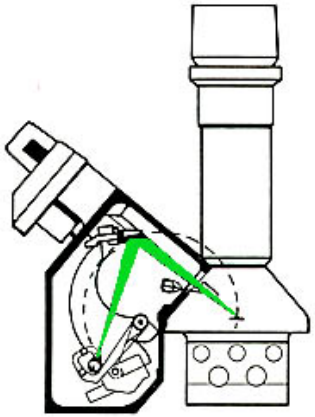

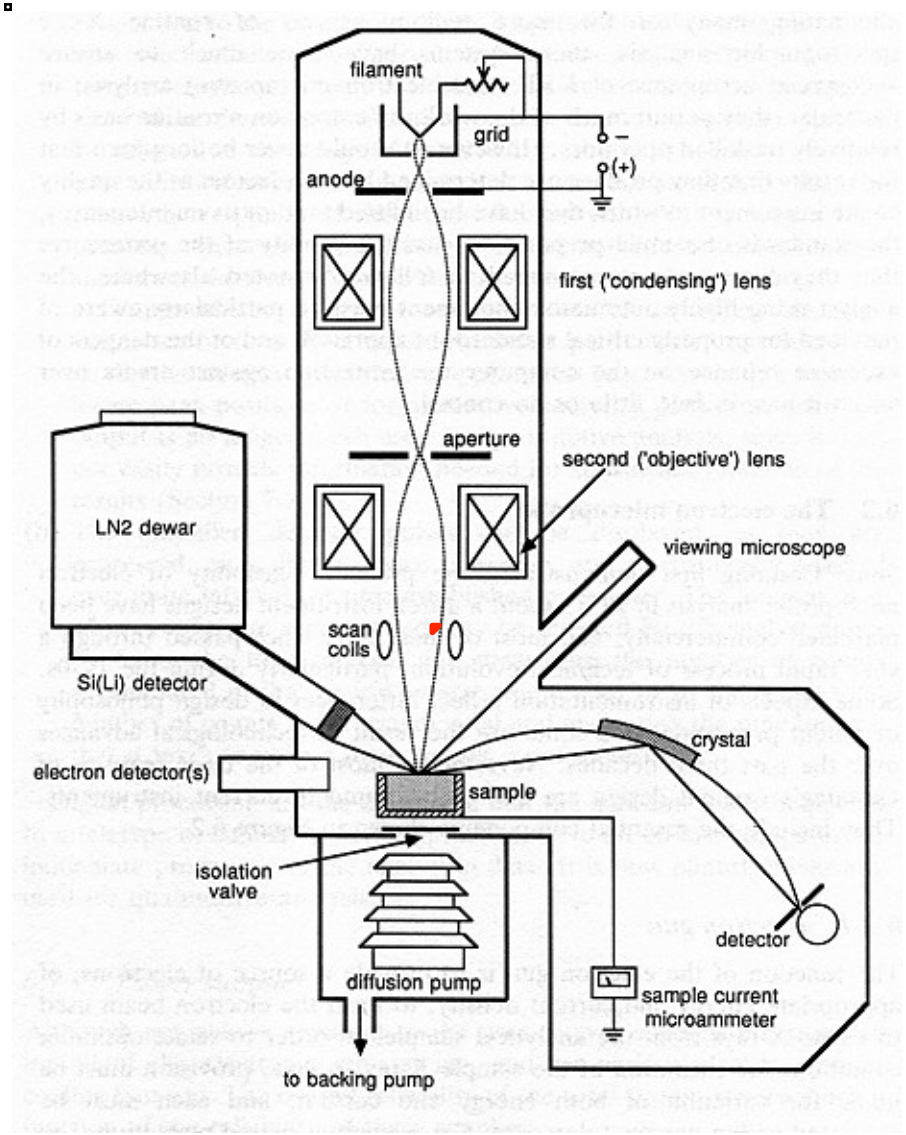

Electron gun

Column/ Electron optics

Optical microscope

Scanning coils

WDS spectrometers

Faraday current measurement

EDS detector

SE,BSE detectors

Vacuum pumps

WDS Spectrometers

An electron microprobe generally has 3-5 spectrometers, with 1-4 crystals in each. Here, SP4 (spectro #4, LF) with its cover off.

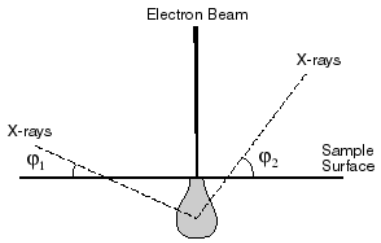

Crystals (2 pairs)

Proportional Counting Tube (note tubing for gas)

PreAmp

$$n\lambda = 2d \sin\theta$$

where, n = an integer (1, 2, 3...),
λ = wavelength,
d = d-spacing of the crystal,
and θ = incident angle (measured from crystal surface)

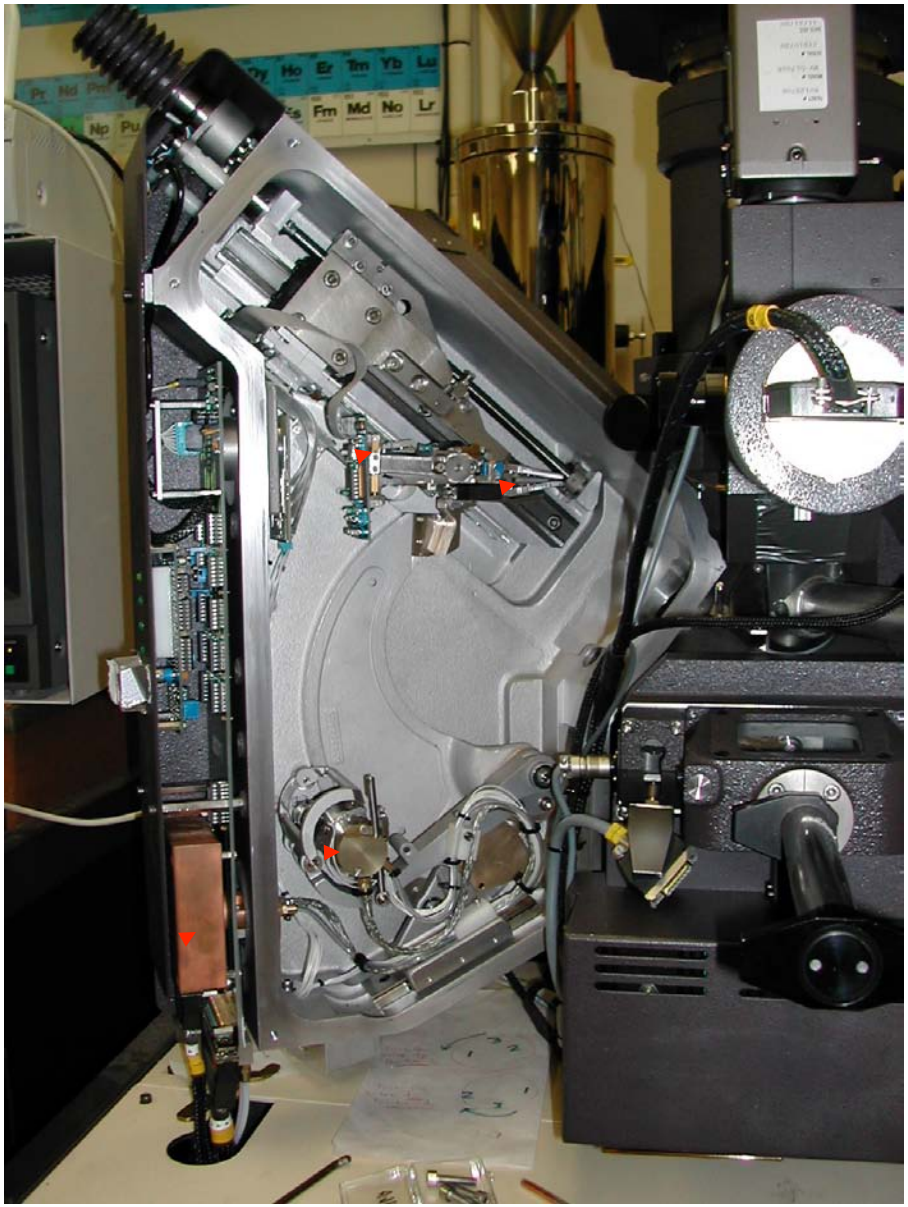

$N\lambda = 2d\sin\theta$

Lots of Analyzing Crystals

Over the course of the first 30 years of EPMA, ~50 crystals and pseudocrystals have been used.

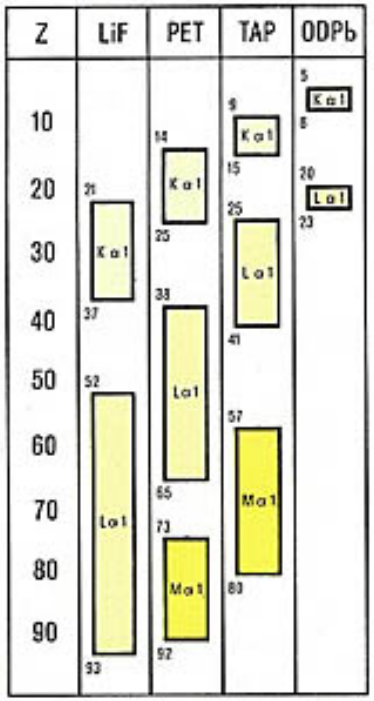

Table 5—Diffracting Crystals for Use in Wavelength Dispersive Spectrometers

Crystal designation and/or crystal name	Reflecting planes	2d spacing (Å)	Approximate useful wavelength coverage in Å	Intensity performance relative to Mica
LiF-lithium fluoride	420	1.78	down to 0.2	
Topaz	303	2.712	-2.5	4.3
SiO_2-quartz	$20\bar{2}3$	2.75	-2.2	2.8
LiF-lithium fluoride	220	2.848		
LiF*-lithium fluoride	200	4.0267	-3.8	12.8
Al-aluminum	100	4.049	0.8-4.3	20.0
SiO_2-quartz	$11\bar{2}0$	4.903	0.8-4.7	1.4
NaCl-sodium chloride	200	5.640	0.9-5.3	15.1
Calcite	104	6.07	1.0-5.7	4.9
ADP-ammonium dihydrogen phosphate	112	6.14	1.0-5.7	
Si-silicon	111	6.2706		
Fluorite		6.2	1.1-5.8	4.1
Ge-germanium	111	6.532	1.1-6.0	6.6
SiO_2*-quartz	$10\bar{1}1$	6.6862	1.1-6.3	5.3
C-pyrolytic graphite	002	6.70		
ADP-ammonium dihydrogen phosphate	200	7.50	1.2-7.3	
SiO_2*-quartz	$10\bar{1}0$	8.492	1.4-8.1	1.5
PET* pentaerythritol	002	8.74	1.4-8.3	11.8
EDDT-ethylene diamine d-tartrate	020	8.808	1.4-8.3	7.4
ADP*-ammonium dihydrogen phosphate	101	10.642	1.8-10.3	3.5
SHA-sorbitol hexaacetate	110	13.98		
Gypsum	020	15.2	2.6-15.0	1.9
BiTitanate		16.40	-16.0	
Ammonium tartrate		14.2		0.2[a]
Ammonium citrate		14.7		0.2[a]
Mica*-muscovite	002	19.84	3.3-19.4	1.0
TLAP-thallium acid phthalate	$10\bar{1}0$	25.9		
RAP-rubidium acid phthalate		26.121	2.0-18.3	
KAP*-potassium acid phthalate	$10\bar{1}0$	26.632	4.5-25.4	6.4
Penninite		28.6		0.2
Chlor-clinochlore	0001	28.392	5. -27.4	0.4
Fe-Mg layered[b]		60	8.3-23.7	
OHM-octadecyl hydrogen maleate		63.5		0.4
Llaur-lead laurate		70	-67	15[a]
LTD[c]-lead tetradeconate		80		
Lmyr-lead myristate		80.5	18-71	
OAO-dioctadecyl adipate		93.8		
OHS-octadecyl hydrogen succinate		96.9		
LSD-lead sterate decanoate		100	17-94	15[a]
LOD*-lead octadeconate		100	17-94	10.7
Fe-Mg layered[d]		104		
LTE[c]-lead tetracosanate		126		
Llign*-lead lignocerate		130	26-120	4[a]
Lcer-lead cerotate		140	31-124	
LTC[c]-lead triacontanate		156		
Lmel-lead melissate		160	35-140	

*Indicates the crystals that have been commonly used in electron probe analysis.
a) Relative intensity related to mica at 13.3 Å by Henke and Lent (Ref. 56); b) 130 alternating layers each of Fe(14Å) and Mg(16Å); c) pseudo-crystal produced by Biodynamics Research Corp., Rockville, Maryland; d) 100 alternating layers each of Fe(13Å) and Mg(39Å).

WDS detector

P10 gas (90% Ar - 10% CH_4) is commonly used as an ionization medium. The X-ray enters through the thin window and 3 things can occur: (1) the X-ray may pass thru the gas unabsorbed (esp for high keV X-rays); (2) it may produce a trail of ion pairs ($Ar^+ + e$), with number of pairs **proportional** to the X-ray energy; and (3) if the X-ray is >3206 eV it can knock out an Ar K electron, with L shell electron falling in its place. There are also 3 possibilities that can result from this new photon:

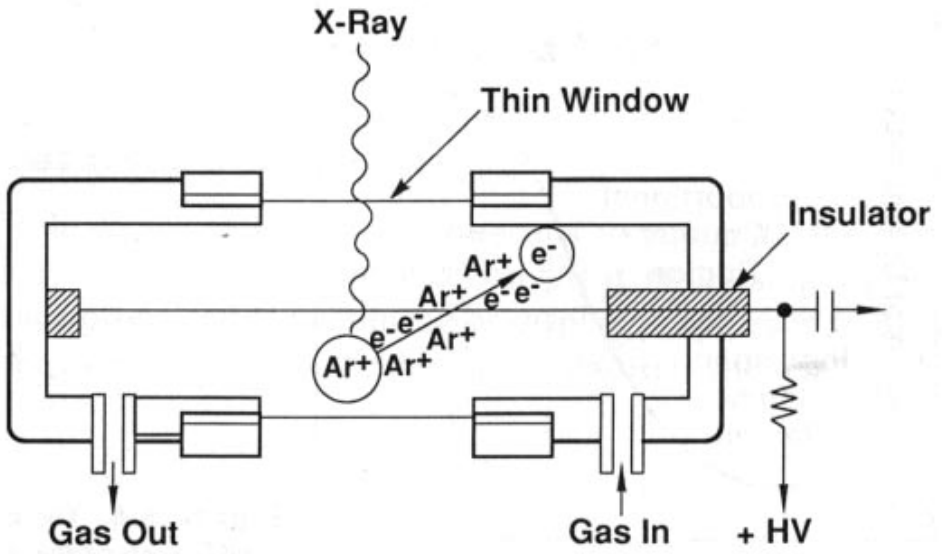

Figure 5.7. Schematic drawing of a gas flow proportional counter.

(3a) internal conversion of the excess energy with emission of Auger electron (which can produce $Ar^+ + e$ pairs); (3b) Ar Ka X-ray itself can knock out electron of another Ar molecule, producing $Ar^+ + e$ pair; or (3c) the Ar Ka X-ray can escape out thru a window, reducing the number of $Ar^+ + e$ pairs by that amount of energy (2958 eV)

2. Li Drifted Si, energy dispersive

Li acts as donor to compensate for impurity acceptor levels (B)
- results in intrinsic region in which $e^- - h^+$ can only be created by external ionizing radiation.
- bias the detector to drag e^- to 1 side.

X ray absorbed in intrinsic layer, E_x

$e^- - h^+$ pairs produced $= \frac{E_x}{\epsilon}$ — 3.7eV in Si

$\therefore$ charge collected $Q = \left(\frac{E_x}{\epsilon}\right) \cdot e$

detector has capacitance, so we actually get a voltage pulse $V = \frac{Q}{C} = \frac{e}{C}\left(\frac{E_x}{\epsilon}\right)$

pulse ht $\propto$ X ray energy $\rightarrow$ energy dispersive
we count pulses (one at a time)

assuming Poisson statistics for Q then $\sqrt{N}$

stand. dev. of voltage pulse is $\Delta V = \frac{e}{C}\sqrt{\frac{E_x}{\epsilon}}$

not Poisson exactly $\Delta N < \sqrt{N}$

$\therefore \frac{\Delta V}{V} = \frac{\frac{e}{C}\sqrt{\frac{E_x}{\epsilon}}}{\frac{e}{C}\left(\frac{E_x}{C}\right)} = \sqrt{\frac{\epsilon}{E_x}}$ $\left(\frac{\sqrt{N}}{N}\right)$

$\therefore \frac{\Delta E_x}{E_x} = \sqrt{\frac{\epsilon}{E_x}} \Rightarrow \boxed{\Delta E_x = \sqrt{\epsilon E_x}}$ energy res.

for a Gaussian distrib: FWHM $= 2.36\,\Delta E_x$ //

X Ray Anal (cont)

call $\frac{\text{St. dev}}{N} = F \Rightarrow$ for Poisson, $F = 1$

F = Fano factor — for Si(Li) = .12 ←

$\therefore \boxed{\Delta E_x^{Si(Li)} = 1.6\sqrt{E_x} \text{ in eV}}$ ←

↳ intrinsic energy resolution

but pulses are small, need amplification

$\therefore$ extra elec. noise

$$\Delta E_{FWHM} = \sqrt{(1.6\sqrt{E_x})^2 + E_{elec\,noise}^2}$$

($E_{elec} \sim 50-100$ eV //

// need to cool to liq N_2 to reduce thermal noise

efficiency of detector:

1) solid X

2) window, metalization layer, dead layer etc..

↳ all of these depend upon the X ray energy

2 effects:

1) X ray absorption in these layers resulting in fewer $e^- - h^+$ produced

2) X rays of high enough energy don't get absorbed in the intrinsic layer

this is similar for all EDX type detectors —

X Ray Analysis (cont)

consider the effluences resulting from these various layers

$$f_{\substack{DET \\ ABS,\ trans}} = \left[\prod_i e^{-(\mu/\rho)_i (\rho t)_i}\right] \times \left[1 - e^{-(\mu/\rho)_A (\rho t)_x}\right]$$

product of absorption in each layer

probability that A xray will be absorbed in intrinsic region

NOTE: if we calc for a layer of given thickness t, we can do any thickness t' as

$$t' = Nt \Longrightarrow e^{-Nt} = (e^{-t})^N \;///$$

it is clear that to minimize absorption in front layers, want to make them as thin as possible.

best is "window less" detector — no vacuum window barrier // probs.

pt. to note /— light element detection is poor since xray energies are so low — any kind of physical window cuts down on transmission.

due com trans. chars of diff. det. materials

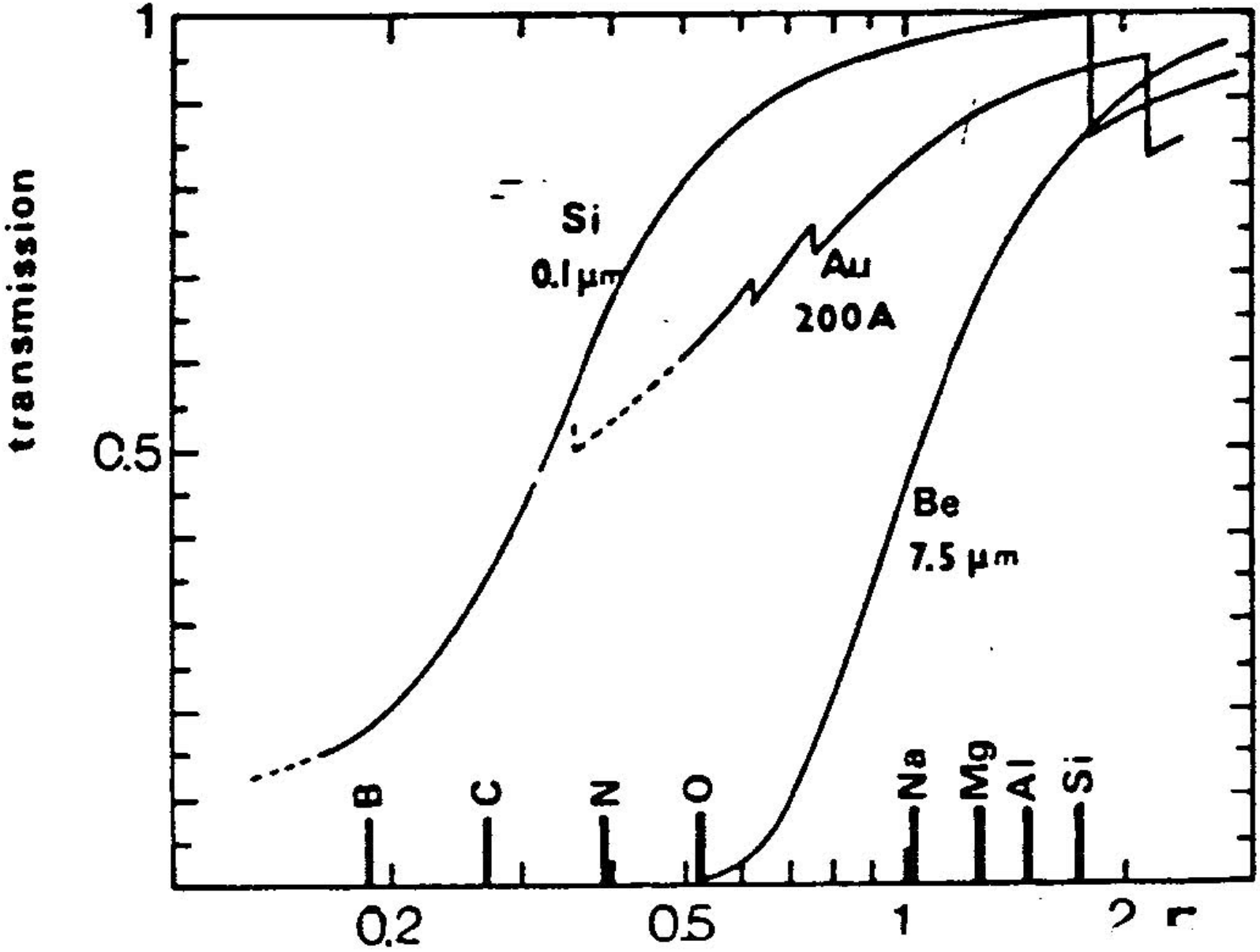
transmission
1
0.5
Si
0.1 μm
Au
200 A
Be
7.5 μm
B
C
N
O
Na
Mg
Al
Si
0.2
0.5
1
2
Xray Energy (in KeV)

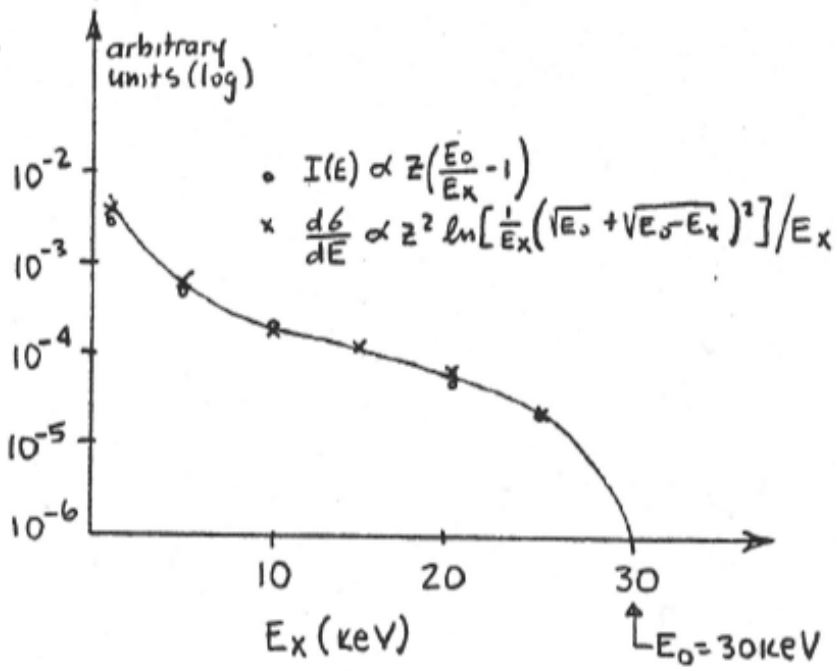

23.2
JJ

results normalized at 15 keV

$I(E)$ → solid target emission (Kramers, 1923)

$\frac{d\sigma}{dE}$ → semi-classical electron slowing down (Jackson, 1962)

— Figure 2. —

Continuum Radiation from charged particles

$$\left(\frac{d\sigma}{dE}\right)_{Br} = \frac{3.2\times10^{-27} Z^2 z^4}{\beta^2}\left(\frac{M_E}{M}\right)^2 \frac{\ell n\left[\frac{1}{E_x}\left(\sqrt{E_0} + \sqrt{E_0 - E_x}\right)^2\right]}{E_x} \quad \text{in cm}^2/\text{eV} \qquad (1$$

where $\beta = v/c$, M_E is the electron mass, Z is the atomic number of the target atom, z is the atomic number of the incident particle. For electrons as the colliding particle, this reduces to:

$$\left(\frac{d\sigma}{dE}\right)_{Br} = \frac{3.2\times10^{-11} Z^2}{\beta^2} \frac{\ell n\left[\frac{1}{E_x}\left(\sqrt{E_0} + \sqrt{E_0 - E_x}\right)^2\right]}{E_x} \quad \text{in Å}^2/\text{eV} \qquad (2$$

The point to be noted here is that this cross-section (per atom) is orders of magnitude smaller than that of the cross-section for characteristic xray production [for the incident electron energies that we will generally be using for microanalysis]. However, if the number concentration of the atoms giving the characteristic xray signal is small, then this cross-section can be of comparable magnitude to the characteristic cross-section, thus affecting the detectability.

considerations on fundamental bkg. in ebeam induced Xray spectra

doc cam
real spectrum

- Jackson, Classical EM - semiclassical (1962) chap #15.
  evaluate using classically
  assume radiation emitted by a charged particle in a Coulomb collision.
- QM taken into account by
  ~~take~~ taking inc ~~ele~~ particle velocity
  to be avg betwn and after collision
  ie. $v_{AVG} = [\sqrt{E_0} + \sqrt{E_0 - E_x}]/2M$

doc cam. real compared to theo

$\beta = \frac{v}{c}$

his result:

$$\left(\frac{d\sigma}{dE}\right)_{Br} = \frac{3.2 \times 10^{-11} Z_T^2}{\beta^2} \frac{\ln\left[\frac{1}{E_x}\left(\sqrt{E_0} + \sqrt{E_0 - E_x}\right)^2\right]}{E_x} \text{ in } \text{Å}^2/\text{eV}$$

---

the "background" for electrons

background limits what we can detect with XRays

note

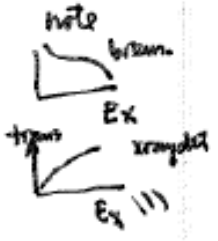

for any charged particle

$$\left(\frac{d\sigma}{dE}\right)_{Br} = \frac{3.2 \times 10^{-11}}{\beta^2} Z_T^2 Z_I^2 \left(\frac{M_e}{M}\right)^2 \frac{\ln[\quad]}{E_x}$$

Z_T = Z of target atoms

Z_I = Z of inc. particle

M_e = ele. mass

M = mass of the incident charged particle

Note // we reduce by going to higher energies or by using incident particles of higher mass than M_{elec} !

what is the min conc. we can detect with X rays //
charged particle induced X rays

peak signal (cts) = $S_A\tau = N_A J \sigma_A Y_A F_A \cdot \tau$ ← count time

from atom type A

$$S_A\tau = \left(\frac{M_A}{A_A m_p}\right) J \sigma_A Y_A F_A \tau = P_A$$

(A_A: at wt; m_p: proton mass)

bkg signal (cts) = $S_{Br}\tau = \frac{M_T}{A m_p} J\left[\left(\frac{d\sigma}{dE}\right)_{Br} \Delta E\right] \cdot F = P_{BACK}$, $Y = 1$ why?

(M_T: total mass; A: avg A of sample; ΔE: energy window)

∴ condition for detection

$P_A \geq K \times \sqrt{P_{BACK}}$ // IF $\frac{S}{N} = \sqrt{N}$ Poisson stats

K = contrast factor – from Rose.

∴ take the two eqns: 1st for M_A, 2nd for M_T

get detectable mass fraction = $MF = \frac{M_A}{M_T} = K \frac{A_A}{\sigma_A Y_A} \left[\frac{m_p}{A M_T} \frac{\left(\frac{d\sigma}{dE}\right)_{Br} \Delta E}{J \tau F}\right]^{1/2}$

2 pts // to decrease MF //

1. Increase Y_A, F
2. decrease $\left.\frac{d\sigma}{dE}\right|_{Br}$
3. increase τ
4. decrease ΔE

Detectable Mass Fraction

Xray detection, EDX

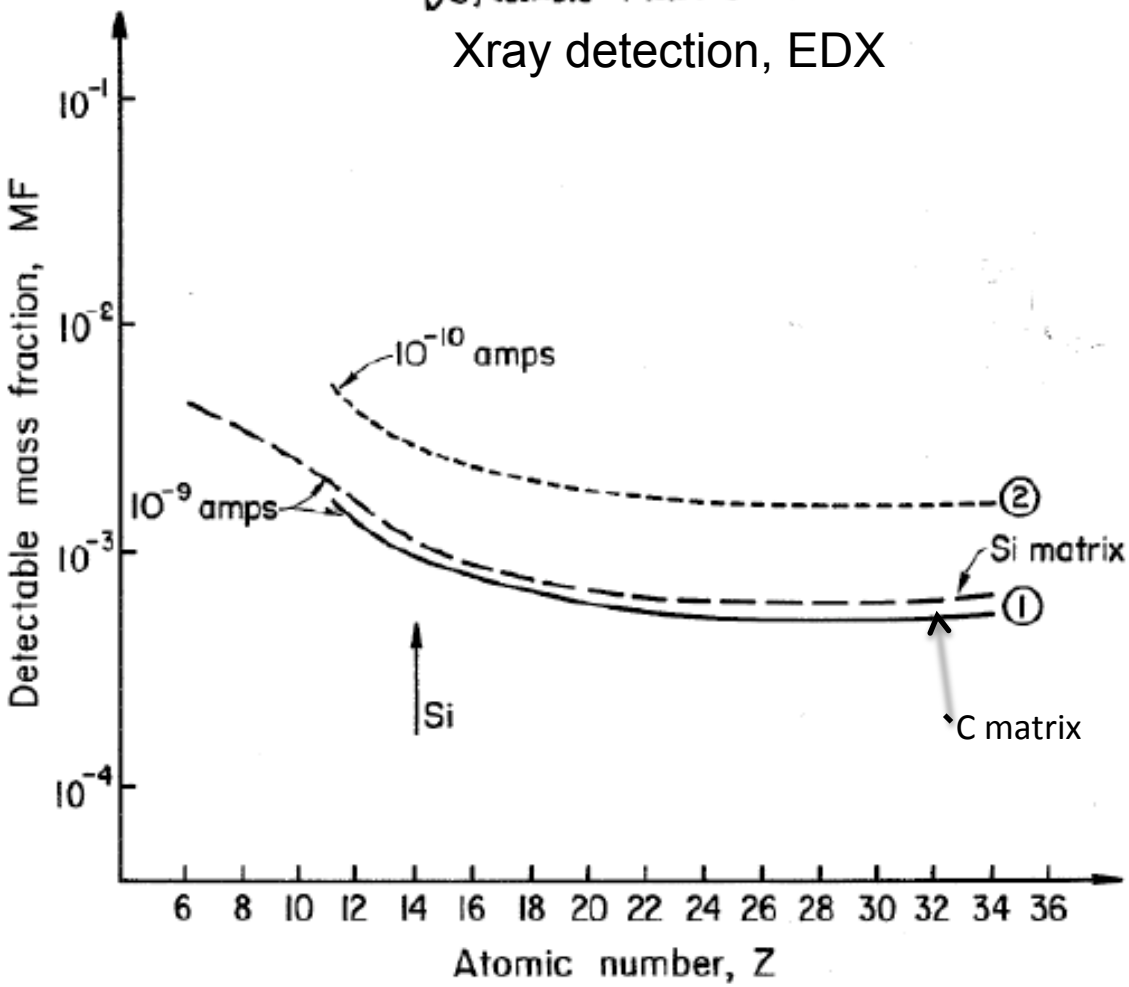

E_0 = 100 KeV, ΔE = 150 eV, τ = 100 sec, K = 3

① d_β = 1 nm, ② d_β = 10 nm

$T_{SUBSTRATE}$ = 100 nm

so what strategy to reduce min. det. conc.

- Note/ $M_T J = \left[\frac{\pi}{4} d_B^2 \rho t\right]\left[I_p / \frac{\pi}{4} d_B^2\right]$

$= \rho t I_p$ — decreasing beam size doesn't reduce MF

but increasing I_p does reduce MF.

- increasing the counting time, ↓ reduces MF
- $\frac{\Delta E}{F}$ reduction helps — depends on detector
- increasing γ_A helps — depends on process we choose
- $\left(\frac{d\sigma}{dE}\right)_{BT} \propto \frac{1}{\beta^2} \frac{1}{(M_{INC})^2}$ so increasing the velocity of the particle or increasing its M_{INC} helps also //

we will discuss all of these —

1. detectors
2. γ_A → if you detect energy for electrons rather than x rays, $\gamma_A = 1 > \omega_a$
3. If you use protons or ions M_{INC} ↑ so MF ↘
4. higher energies help somewhat since $\frac{d\sigma}{dE}\Big|_{BT} \propto \frac{1}{N^2}$ but so does $\sigma_{section}$ — so not so big an effect

SCATTERING MECHANISMS FOR CHARACTERIZATION

1. UNSCATTERED
   $\Delta E = 0,\ \Delta P = 0$

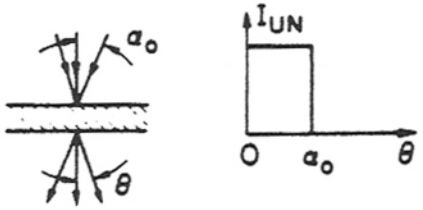

2. ELASTICALLY SCATTERED
   $\Delta E \approx 0$
   $\sigma_{EL} \sim Z^{3/2}$
   $\theta_0 \sim \lambda / 2\pi a \gtrsim \theta_B$

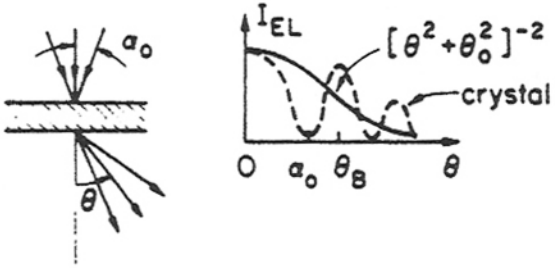

3. INELASTICALLY SCATTERED
   $\theta_E \approx \frac{\Delta E}{P_0 V_0}$
   $\sigma_{IN} \sim Z^{1/2}$
   $\frac{d\sigma_{IN}}{dE}$ material specific

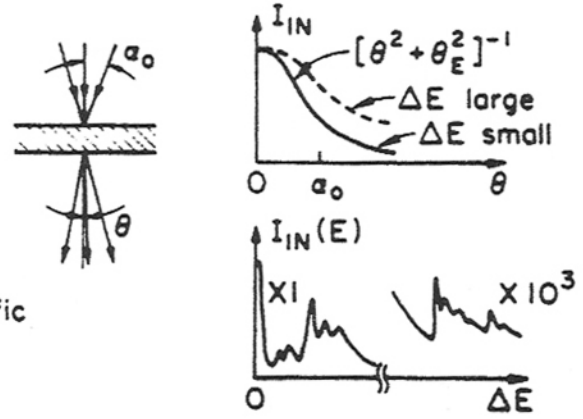

EELS of Nucleic Acid Bases obtained Using 25keV Incident Electrons

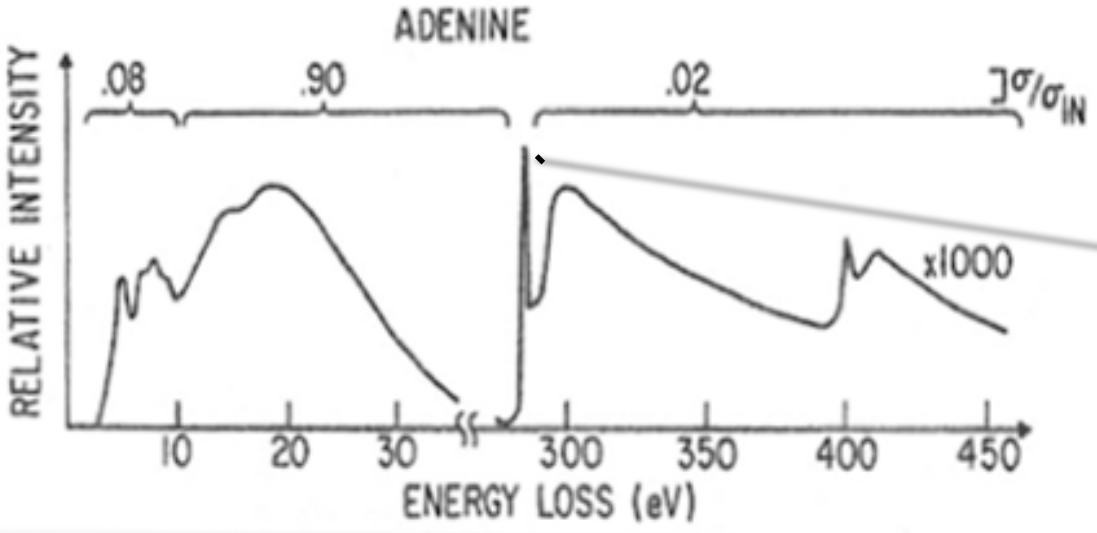

M.Isaacson, D.Johnson and A.V.Crewe. , Rad. Res.55 (1973).205.

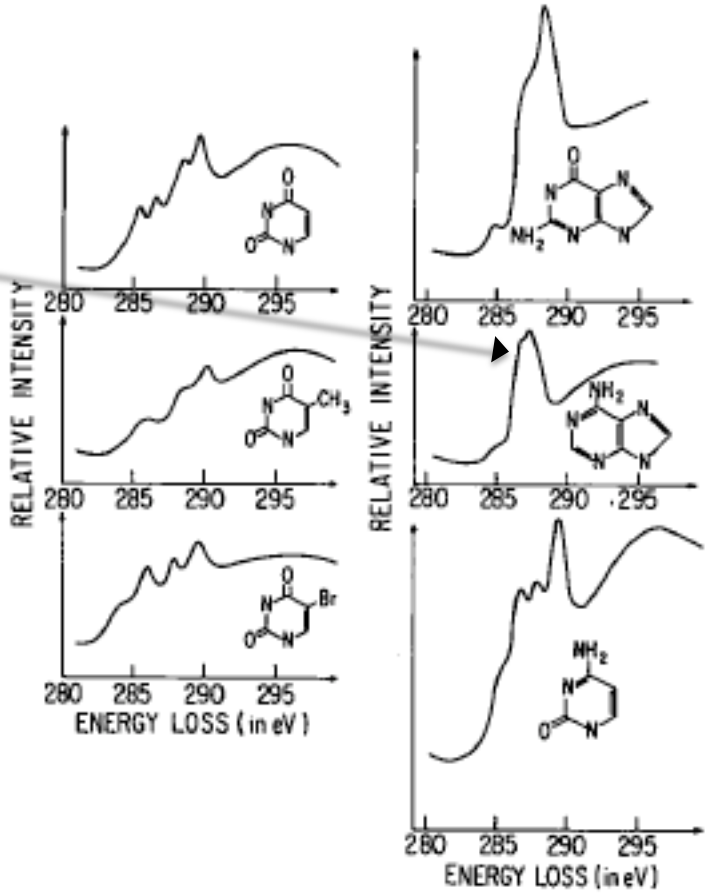

M.Isaacson and D. Johnson, Ultramicroscopy.1 (1975).33-52.

Energy Loss Spectra of Metal Fluorides

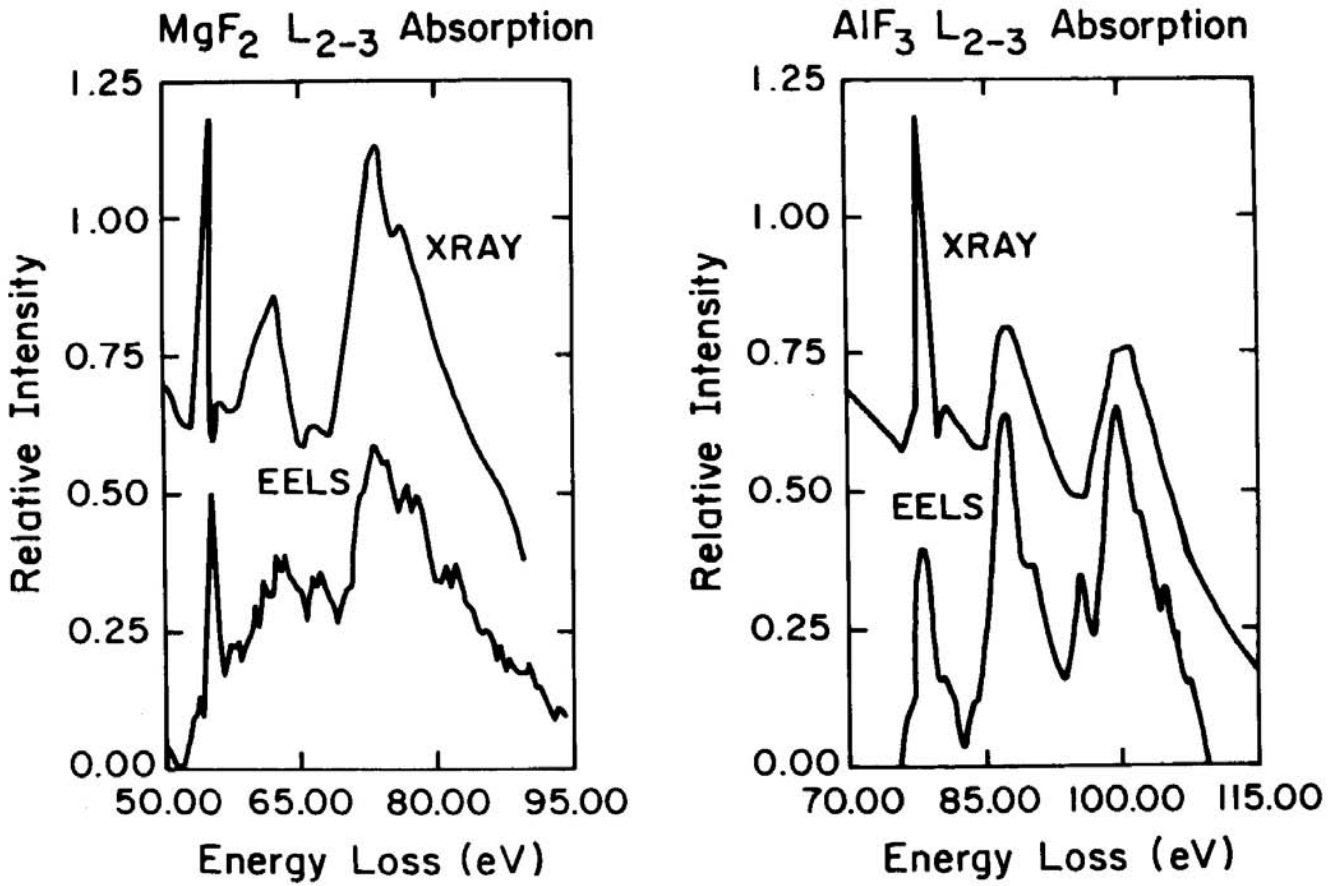

M. Scheinfein and M. Isaacson, J.Vac.Sci.Tech.B4(1) 1986. 326 – 332.

How to Measure Energy of Energy Loss Electrons?

fn X Rays, solid state detectn

energy deposited $\Rightarrow$ e^-h pairs
creates voltage pulse

$\Delta E \approx 1.6\sqrt{E_x}$ resolution

resolution $\sim$ 100 eV //

if we used same fn electrons,
incident energy $\sim 10^2$ keV (in an EM)
if energy lost is 1keV, then
99 keV electron hits detector.

$\therefore \Delta E \sim 1.6\sqrt{99\times10^3} \cong 500$ eV // !

so we resort to $\vec{E}$, $\vec{B}$ fields which deflect the electrons — and separate different energies in space.

$$\vec{F} = Q(\vec{v}\times\vec{B} + \vec{E})$$

more on this later, but can get $\Delta E/E \sim 10^{-6}$!

Rutherford Scattering (coulomb scatt)

Phil. Mag. 21. 669 (1911)

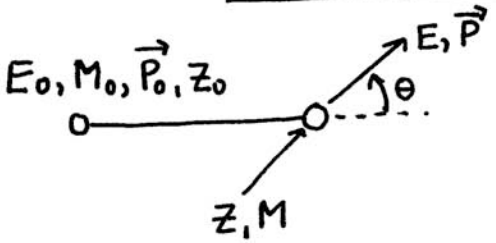

$$\frac{d\sigma}{d\Omega} \propto \frac{(eZ_0)^2(eZ)^2}{E_0^2}\left[\frac{4\left(\cos\theta+\sqrt{1-X^2\sin^2\theta}\right)^2}{\sin^4\theta\sqrt{1-X^2\sin^2\theta}}\right]$$

where $X = M_0/M$ same for RBS

for electrons $X \ll 1$ and $Z_0 = 1$

$$\therefore \frac{d\sigma}{d\Omega} \propto \frac{e^4 Z^2}{E_0^2}\frac{1}{\sin^4(\theta/2)}$$ OK for larger θ

for electrons / Ruth Scatt ~ elastic
ie, virtually no energy loss —

$$\Delta E_{MAX} \cong \frac{4m_e}{M}E_0$$ max. energy that can be transferred in collision

$\frac{m_e}{m_p} = 5.46\times10^{-4}$ | eg, 100keV electrons
iron, A=55.8 amu
$\therefore \Delta E_{MAX} \cong 3.9$ eV

Knock-on Damage

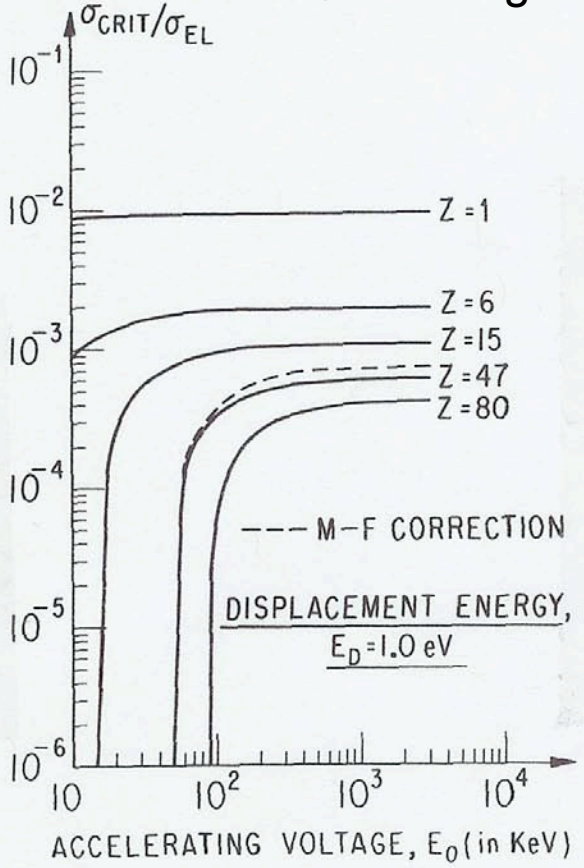

(B)

Fig. 1.3 (*Continued*)

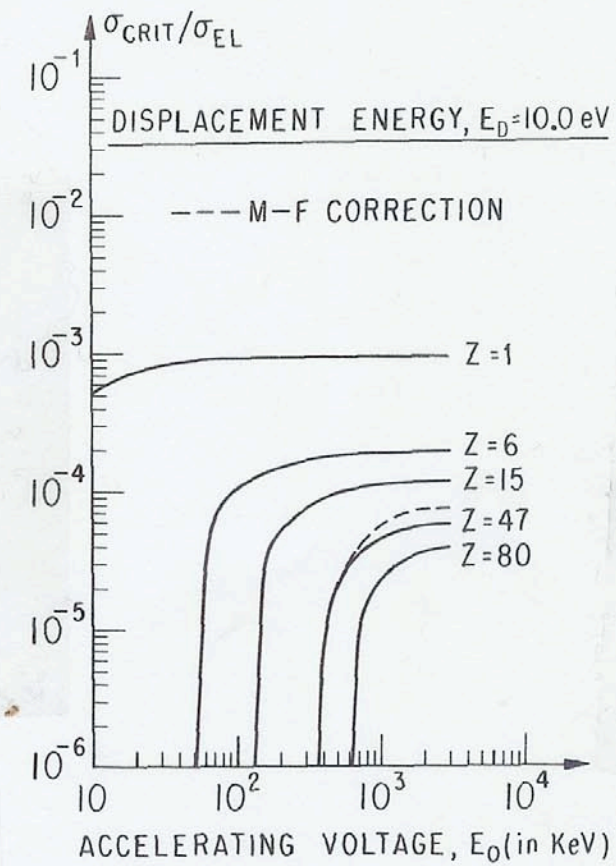

(C)

Fig. 1.3 (*Continued*)

$$\sigma_{CRIT}/\sigma_{EL} \cong \left(\frac{\lambda}{4\pi a}\right)^2 \left[\frac{E_M}{E_D} - 1\right]$$

from M. Isaacson. in Princ. & Tech. of Electron Microscopy. Vol. 7 (ed. M.A. Hayat, Van Nostrand) chap. 1. pg 1-70. (1977).

Minimum Detectable Concentration, EELS

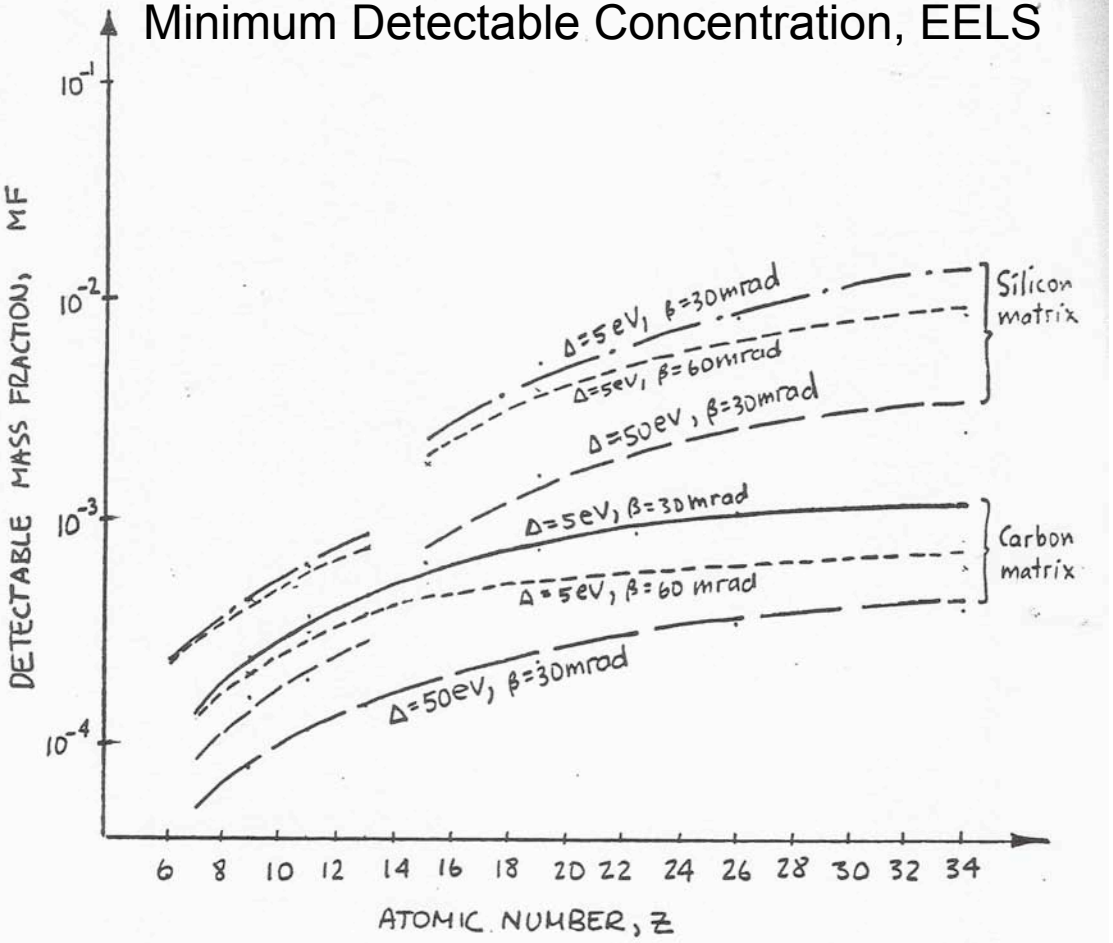

figure 3.

detectable mass fraction $MF = K A_A \left[\frac{m_p \sigma_B F_B}{\bar{A} M J \tau}\right]^{1/2} \frac{e^{nT\sigma^{1/2}}}{\sigma_p F_p}$

We assume 100 keV incident electrons. Sample is 1000 Å thick.

All curves assume $K=3$, $J_B = 1.27 \times 10^5$ Amps/cm^2 ($I_B = 10^{-9}$ Amps, $d_B = 10$ Å) and $\tau = 100$ sec.

Single Atom Identification in STEM

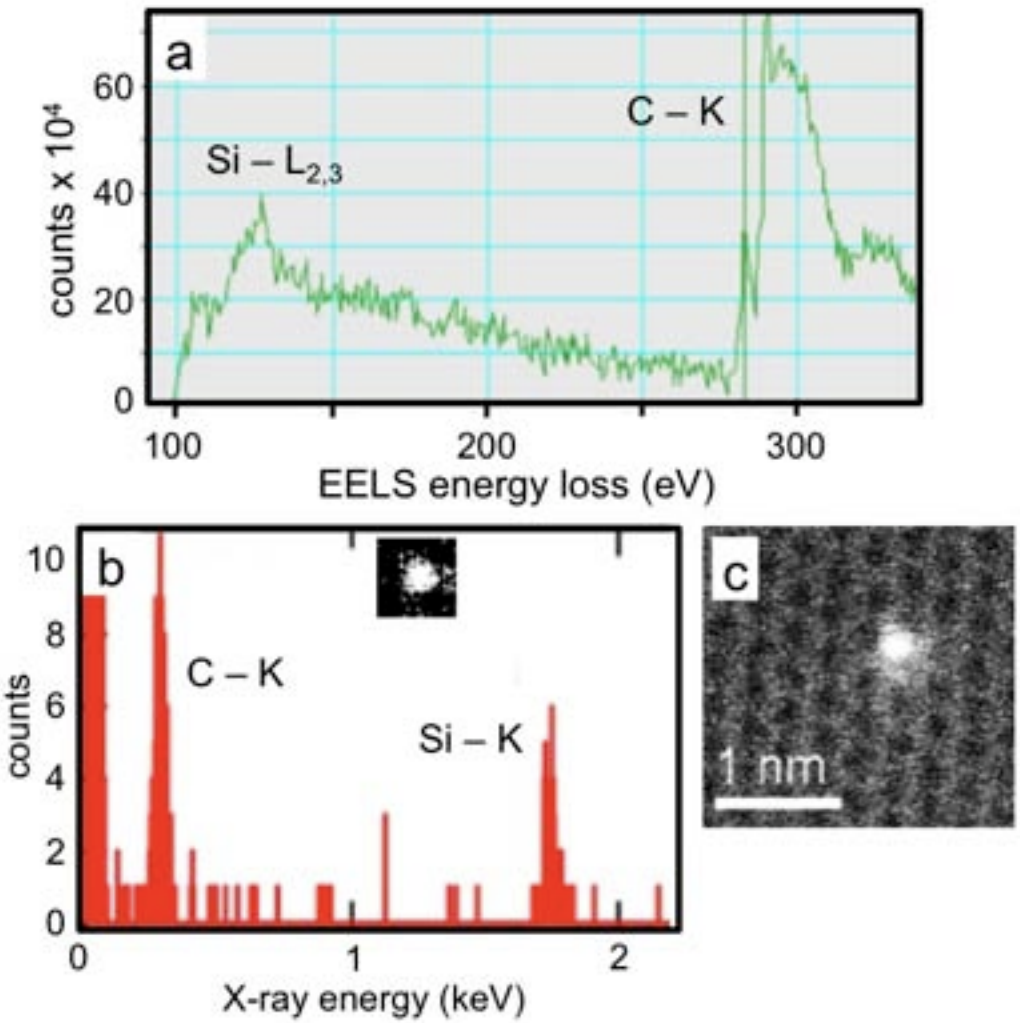

From O. Krivanek, et.al. Ultramicroscopy. (2012).in press

STEM Imaging/EELS of individual atoms/defects

From Krivanek, et.al. Ultramicroscopy.(2102) In press

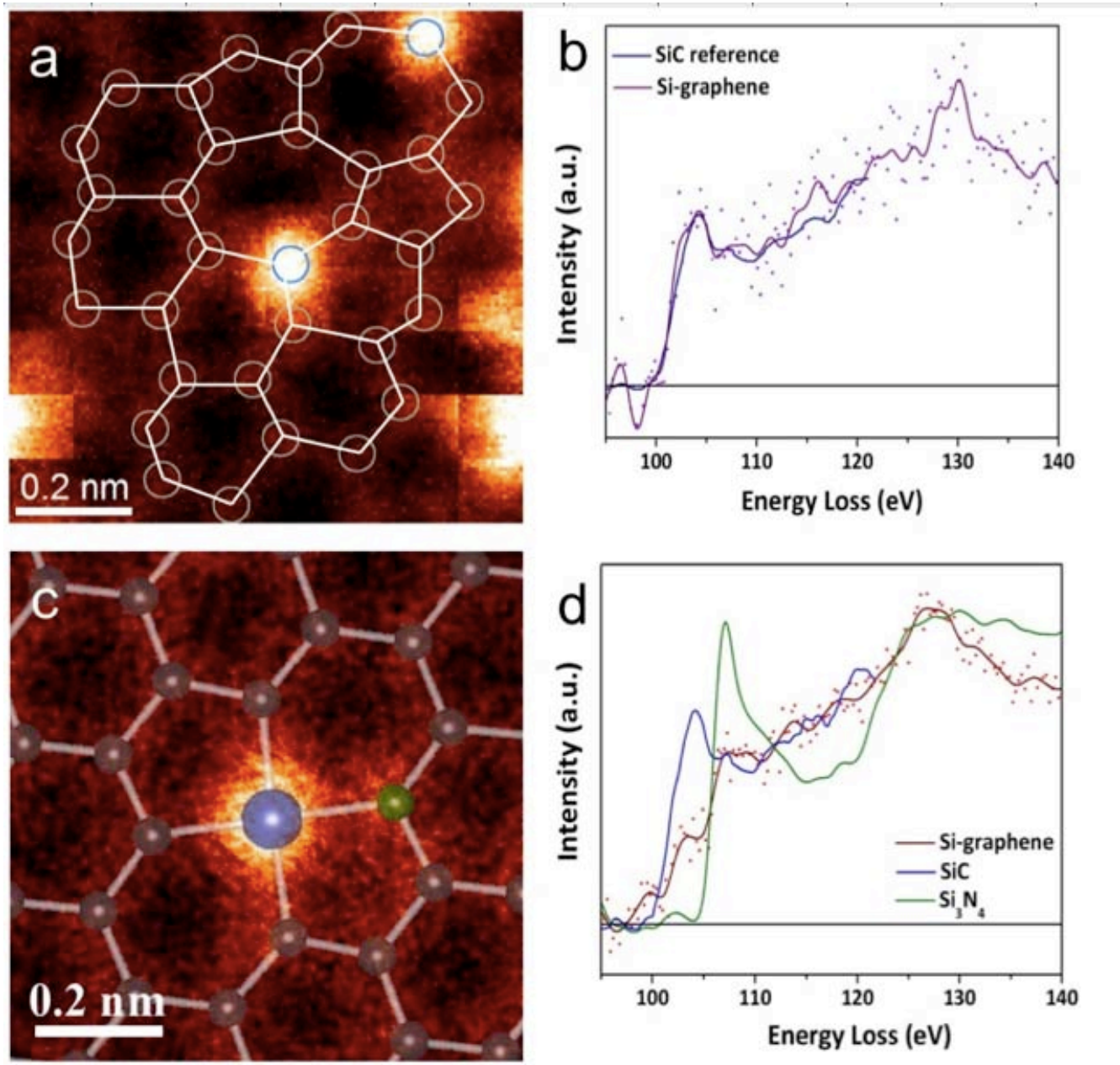

Single Atom
Detection by EELS

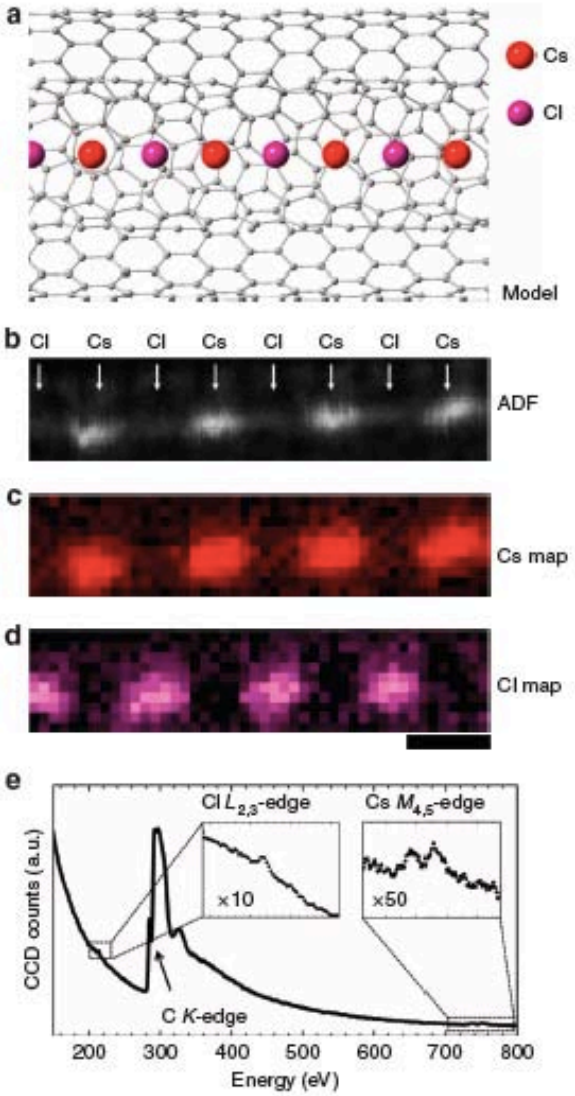

Figure 3 | Detection of single Cl atoms. (**a**) Atomic model of a CsCl atomic chain inside a DWNT. (**b**) An ADF image of a CsCl atomic chain. (**c**,**d**) EELS chemical maps for the Cs *M*-edge and Cl *L*-edge corresponding to **b**, respectively. (**e**) An EELS spectrum of the CsCl atomic chain in **b** showing a trace of Cl and Cs, as well as the carbon *K*-edge which corresponds to the DWNT. The ADF image **b** only shows the Cs atomic positions as bright spots which are consistent with the red spots in the EELS chemical map of the Cs *M*-edge **c**. The EELS map for the Cl *L*-edge **d** clearly shows the existence of Cl atoms in between Cs atoms despite of hardly visible ADF contrast in **b**. Scale bar, 0.5 nm.

Senga & Suenaga. Nature Communications. 6.7943 (1915)

so what strategy to reduce min. det. conc.

- Note/ $M_T J = \left[\frac{\pi}{4} d_B^2 \rho t\right]\left[I_p / \frac{\pi}{4} d_B^2\right]$

$= \rho t I_p$ — decreasing beam size doesn't reduce MF

but increasing I_p does reduce MF.

- increasing the counting time, ↓ reduces MF
- $\frac{\Delta E}{F}$ reduction helps — depends on detector
- increasing γ_A helps — depends on process we choose
- $\left(\frac{d\sigma}{dE}\right)_{BT} \propto \frac{1}{\beta^2} \frac{1}{(M_{INC})^2}$ so increasing the velocity of the particle or increasing its M_{INC} helps also //

we will discuss all of these —

1. detectors
2. γ_A → if you detect energy for electrons rather than x rays, $\gamma_A = 1 > \omega_a$
3. If you use protons or ions M_{INC} ↑ so MF ↘
4. higher energies help somewhat since $\frac{d\sigma}{dE}\Big|_{BT} \propto \frac{1}{N^2}$ but so does $\sigma_{section}$ — so not so big an effect

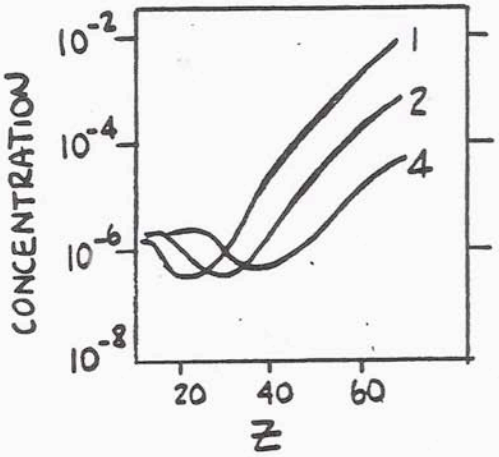

Figure 8.

For ebeam induced Xrays, Concentrations about 0.1-1%

minimum detectable concentration for proton induced xray fluorescence
each solid line corresponds to the proton energy in MeV.

The detectable weight concentration of a trace element of atomic number Z in a 0.1mg/cm² carbon matrix.
The concentration calculated assumes peak counts = $2 \times \sqrt{2 \times \text{background count}}$
The solid angle that the Si(Li) detector subtends is
$\Delta\Omega = .003 \times 4\pi$ ster. We assume 100% detector efficiency.
The incident proton charge is 10 μcoul and the signal detected is Kα xrays.

F. Folkmann, C. Gaarde, T. Huus and K. Kemp. Nuc. Inst. Meth. 116. 487(1974)

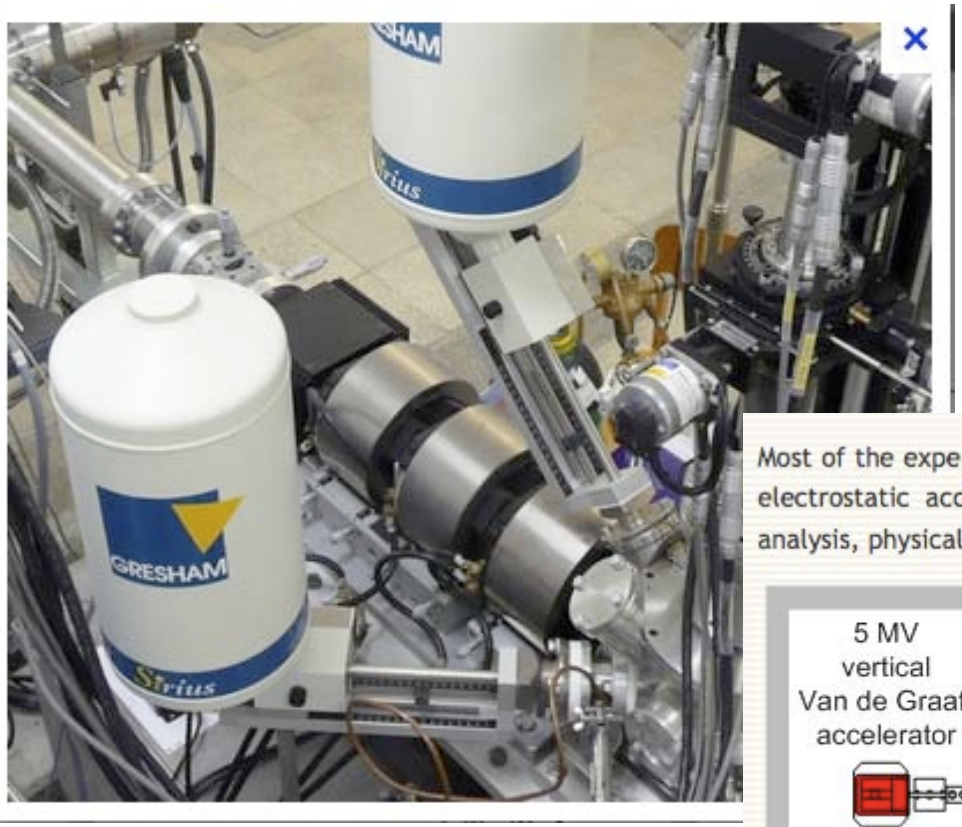

MicroPIXE,

Most of the experimental facilites of our laboratory are based on a 5 MV Van de Graaff (VdG) electrostatic accelerator. VdG provides energetic ions (H+, D+, He+, etc.) for ion beam analysis, physical experiments, as well as for the modification and testing of materials.

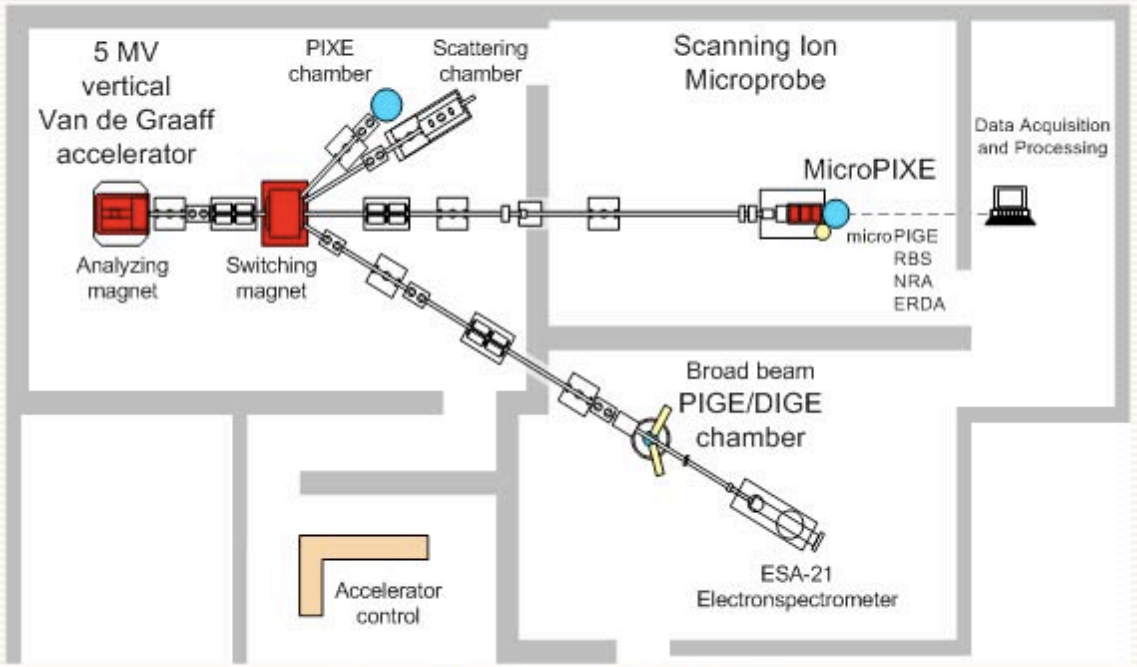

Schematic diagram of the IBA Lab.

http://iba.atomki.hu/facilities.html

Proton Induced X-ray Emission (PIXE)

NAA | PIXE
OC/EC | XAFS
XRF | CHNO

PIXE Applications and Theory

Elemental Analysis Incorporated, utilizing Proton Induced X-ray Emission (PIXE), provides a non-destructive, simultaneous analysis for the 72 inorganic elements from Sodium through Uranium on the Periodic Table for solid, liquid, and thin film (i.e. aerosol filter) samples. The PIXE technique offers the advantage of analysis, without the necessity for time consuming digestion, thereby minimizing the potential for error resulting from sample preparation.

Sample Types

Return to Top

Solids – such as plastics, papers or metals, are analyzed "as received," while powdered materials, such as fly ash, activated carbon, catalysts, and corrosion products, are ground to 200 mesh or finer and pressed into pellets for analysis.

Liquid – samples, such as oils, process waters, and solutions, are analyzed using a plastic cup of either 8 mL or 3 mL in capacity with a 0.3 mil Kapton front surface window, and can be analyzed "as received" by this method without modification. However, some liquids (i.e. highly caustic or highly acidic) may require predilution or neutralization before analysis.

www.eag.com


EAG
Evans Analytical Group
Materials Characterization
简体中文 繁體中文 日本語 Français
Corporate Home
About
Divisions
News
Locations
Specialists in Materials Characterization
1-800-366-3867
Google™ Custom Search
Request Our Services
Home
About
Techniques
Industries
Applications
Publications
News & Events
Get In Touch
30+ METHODS
for Materials
Characterization &
Surface Analysis
Find out which technique is right for you.

NISTIR 5632 | **Version History** | **Disclaimer**

Tables of X-Ray Mass Attenuation Coefficients and Mass Energy-Absorption Coefficients from 1 keV to 20 MeV for Elements Z = 1 to 92 and 48 Additional Substances of Dosimetric Interest*

J. H. Hubbell† and S. M. Seltzer
Radiation and Biomolecular Physics Division, PML, NIST

Abstract

Tables and graphs of the photon mass attenuation coefficient μ/ρ and the mass energy-absorption coefficient μ_{en}/ρ are presented for all of the elements Z = 1 to 92, and for 48 compounds and mixtures of radiological interest. The tables cover energies of the photon (x-ray, gamma ray, bremsstrahlung) from 1 keV to 20 MeV. The μ/ρ values are taken from the current photon interaction database at the National Institute of Standards and Technology, and the μ_{en}/ρ values are based on the new calculations by Seltzer described in Radiation Research **136,** 147 (1993). These tables of μ/ρ and μ_{en}/ρ replace and extend the tables given by Hubbell in the International Journal of Applied Radiation and Isotopes **33,** 1269 (1982).

Note on NIST X-ray Attenuation Databases

Table of Contents

*Work supported by the Standard Reference Data Program of NIST.
†Work carried out for NIST under contract 43NANB412756.

U.S. DEPARTMENT OF COMMERCE - Mickey Kantor, *Secretary*
Technology Administration - Mary L. Good, *Under Secretary for Technology*
National Institute of Standards and Technology - Arati Prabhakar, *Director*

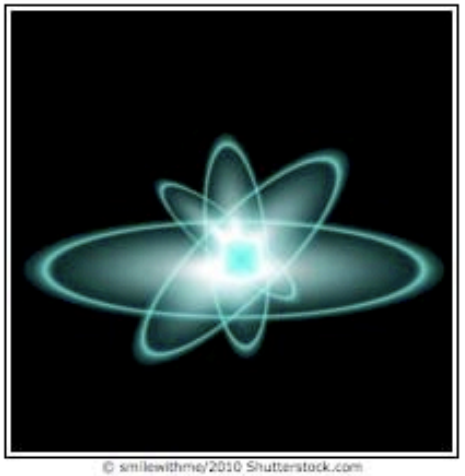

Access the Data for:

Elemental Media

or

Compounds & Mixtures

NIST Standard Reference Database 126
Rate our products and services.
Online: May 1996 - **Last update:** July 2004

Contact

Stephen Seltzer
Radiation and Biomolecular Physics Division
phone: 301-975-5552
fax: 301-869-7682

100 Bureau Drive, M/S 8460
Gaithersburg, MD 20899-8460

http://www.nist.gov/pml/data/xraycoef/

NISTIR 4999 | **Version History** | **Disclaimer**

SHARE

Stopping-Power and Range Tables for Electrons, Protons, and Helium Ions

M.J. Berger,[1] J.S. Coursey,[2] M.A. Zucker[2] and J. Chang[2]

[1]NIST, Physics Laboratory, Ionizing Radiation Division
[2]NIST, Physics Laboratory, ECSED

estar astar pstar

© Creations/2010 Shutterstock.com

Abstract:

The databases ESTAR, PSTAR, and ASTAR calculate stopping-power and range tables for electrons, protons, or helium ions, according to methods described in ICRU Reports 37 and 49. Stopping-power and range tables can be calculated for electrons in any user-specified material and for protons and helium ions in 74 materials.

Contents:

This work was supported in part by the Department of Energy, Office of Health and Environmental Research, Washington, D.C. 20585; and by NIST's Systems Integration for Manufacturing Applications (SIMA) Program.

Access the Data

Electrons | **Protons** | **Helium Ions**

NIST Standard Reference Database 124
Online: October 1998 - **Last update:** August 2005

Contact

Stephen Seltzer
Ionizing Radiation Division
phone: 301-975-5552
fax: 301-869-7682

100 Bureau Drive, M/S 8460
Gaithersburg, MD 20899-8460

RANGE

charged particles:

CSDA Range (continuous slowing down approx, Bethe Range)

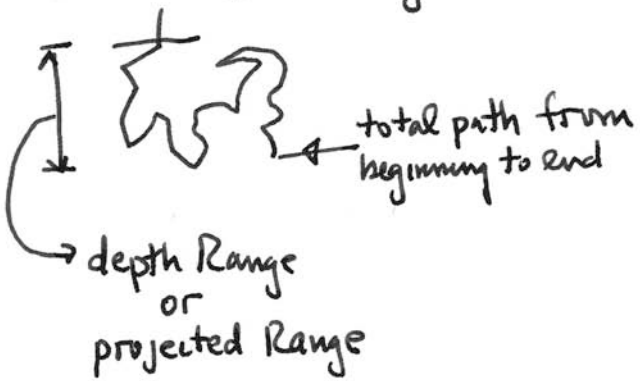

for electrons, proj. Range < CSDA Range

for protons, proj Range ~ CSDA Range

X Rays: μ absorption coefficient

energies we are interested $\lesssim$ 100 KeV

mainly photoeffect — all or nothing

$\therefore \frac{I(t)}{I(0)} = e^{-\mu t}$

so we can think of a projected Range as $R \sim 3/\mu$ ie, $\frac{I(t)}{I(0)} \sim 3 \times 10^{-2}$

PSTAR : Stopping Power and Range Tables for Protons

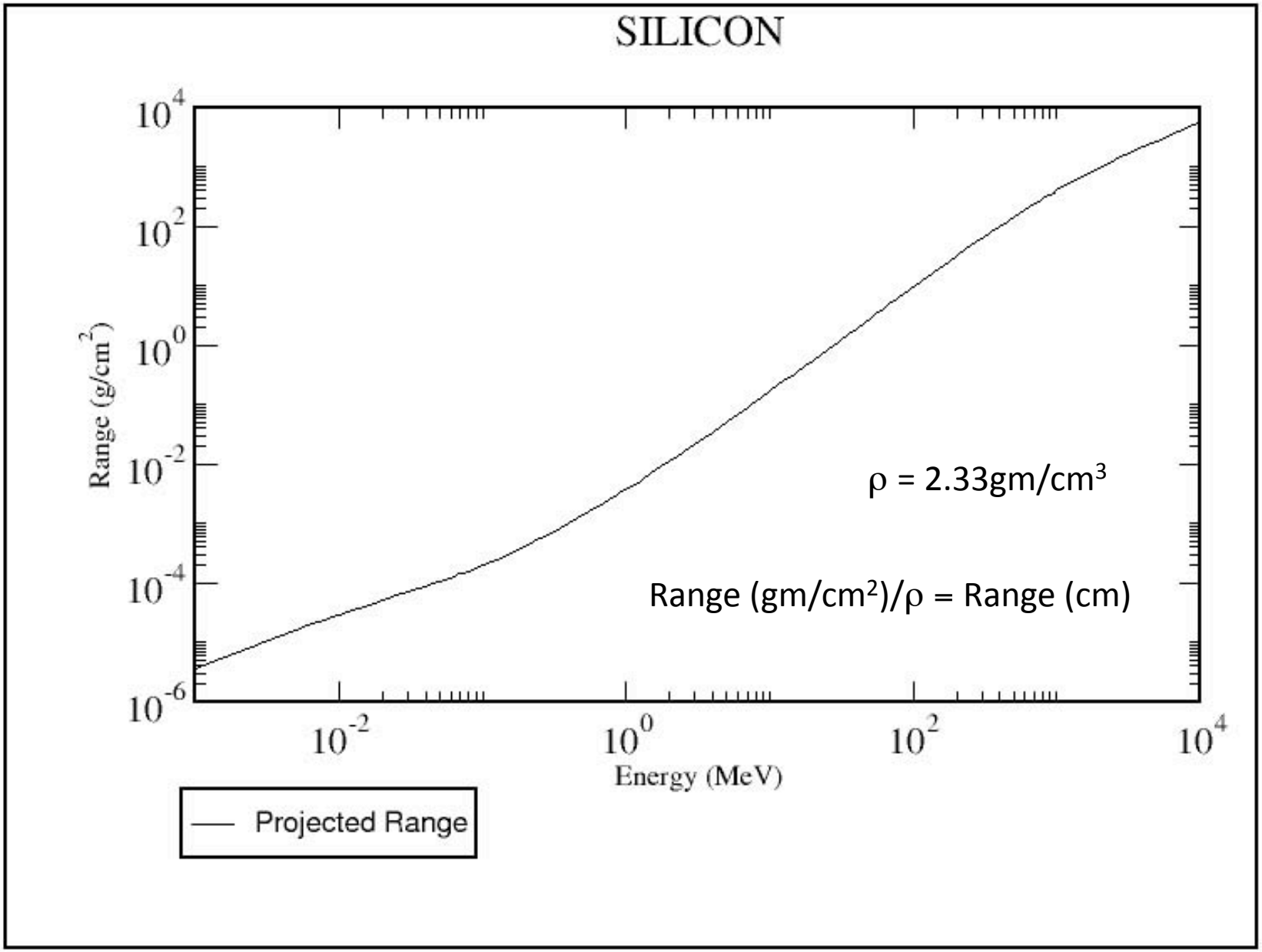

ESTAR : Stopping Power and Range Tables for Electrons

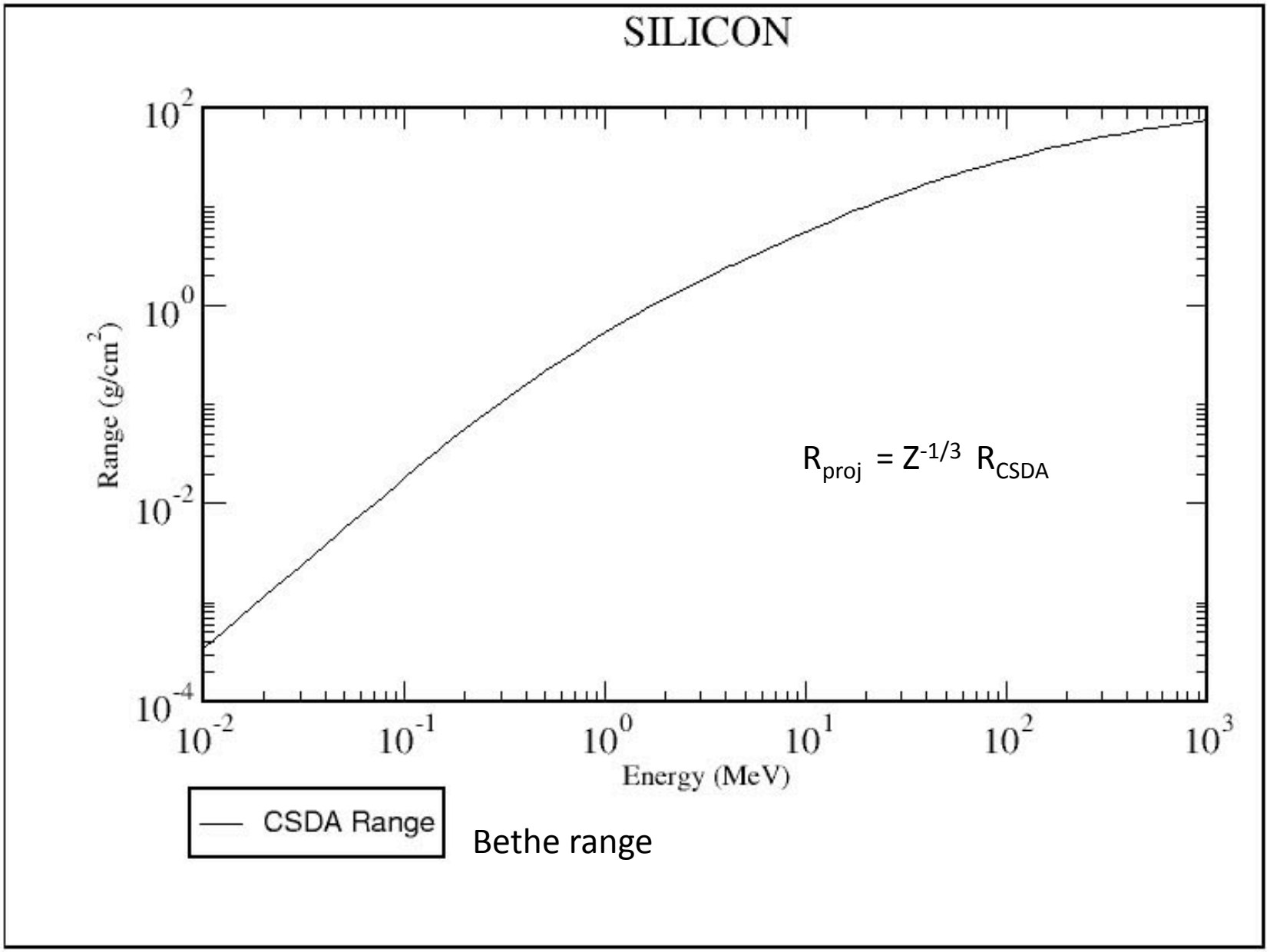

Bethe range

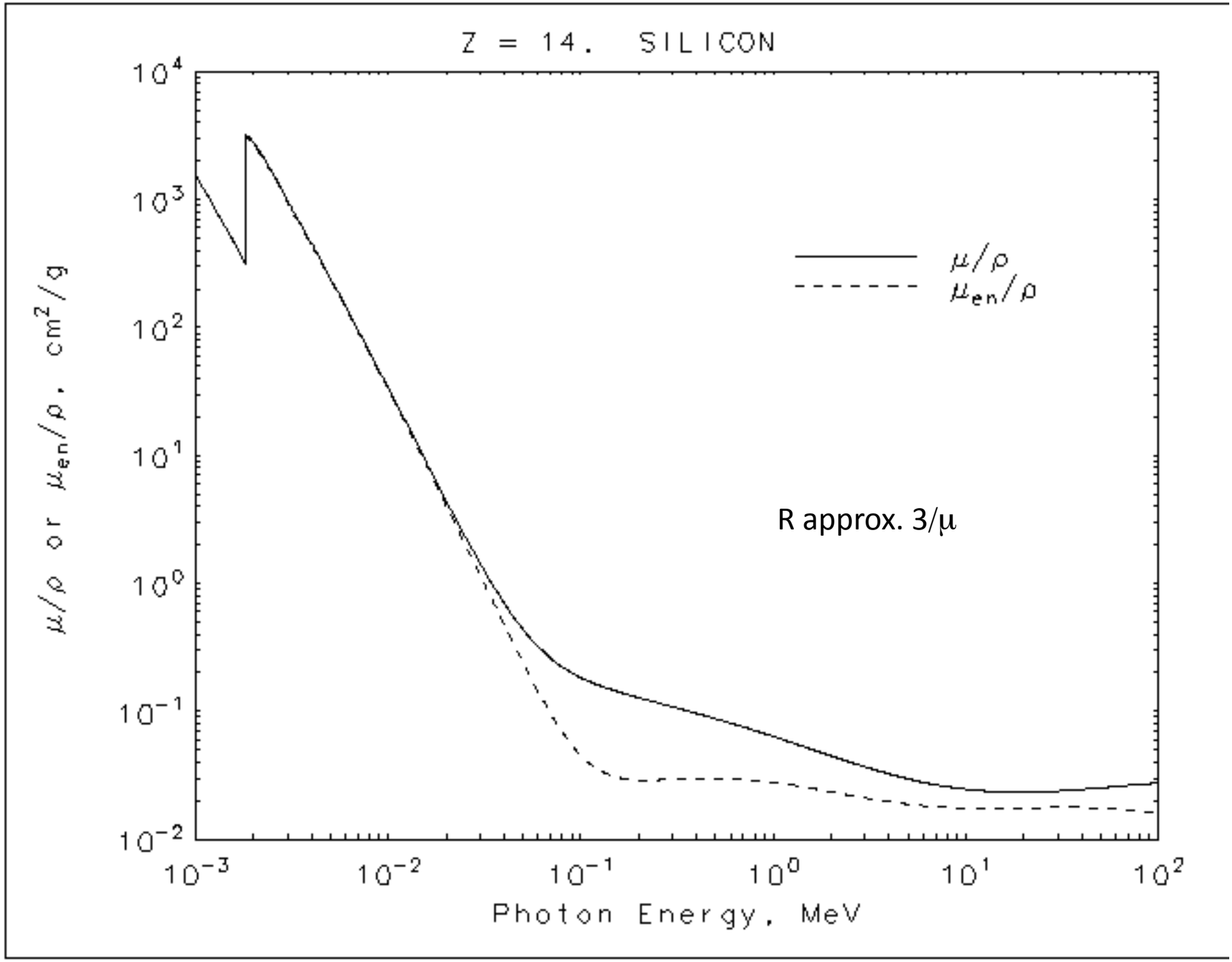
Z = 14. SILICON
μ/ρ
μ_{en}/ρ
R approx. 3/μ
μ/ρ or μ_{en}/ρ, cm^2/g
Photon Energy, MeV
10^4
10^3
10^2
10^1
10^0
10^{-1}
10^{-2}
10^{-3}
10^{-2}
10^{-1}
10^0
10^1
10^2

Comparison of "projected" ranges

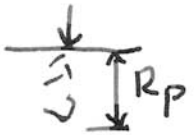

for 100 keV incident

$R_{p\,elec} = Z^{-1/3} R_{CSDA} \longrightarrow 1.78 \times 10^{-3}$ cm

$R_{p\,protn} = R_p \longrightarrow 4.3 \times 10^{-5}$ cm

$R_{p\,XRay} = 3/\mu \longrightarrow 6.44$ cm

Proton Induced X-ray Emission (PIXE)

NAA | PIXE
OC/EC | XAFS
XRF | CHNO

PIXE Applications and Theory

Elemental Analysis Incorporated, utilizing Proton Induced X-ray Emission (PIXE), provides a non-destructive, simultaneous analysis for the 72 inorganic elements from Sodium through Uranium on the Periodic Table for solid, liquid, and thin film (i.e. aerosol filter) samples. The PIXE technique offers the advantage of analysis, without the necessity for time consuming digestion, thereby minimizing the potential for error resulting from sample preparation.

Sample Types

Return to Top

Solids – such as plastics, papers or metals, are analyzed "as received," while powdered materials, such as fly ash, activated carbon, catalysts, and corrosion products, are ground to 200 mesh or finer and pressed into pellets for analysis.

Liquid – samples, such as oils, process waters, and solutions, are analyzed using a plastic cup of either 8 mL or 3 mL in capacity with a 0.3 mil Kapton front surface window, and can be analyzed "as received" by this method without modification. However, some liquids (i.e. highly caustic or highly acidic) may require predilution or neutralization before analysis.

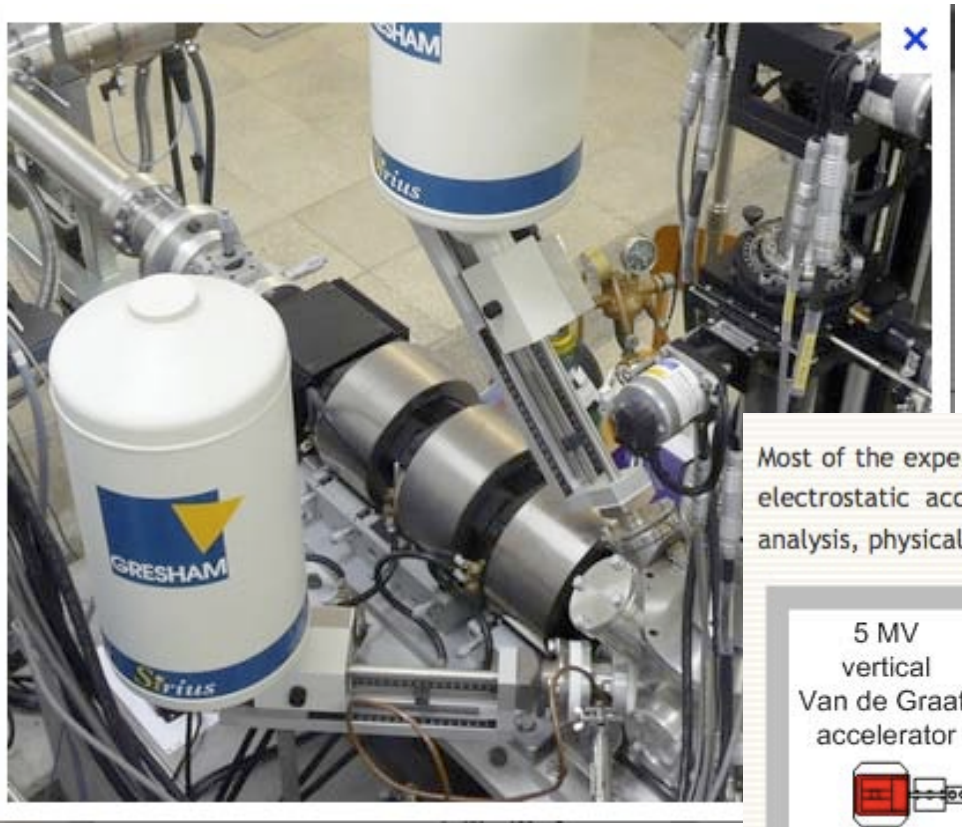

MicroPIXE,

Most of the experimental facilites of our laboratory are based on a 5 MV Van de Graaff (VdG) electrostatic accelerator. VdG provides energetic ions (H+, D+, He+, etc.) for ion beam analysis, physical experiments, as well as for the modification and testing of materials.

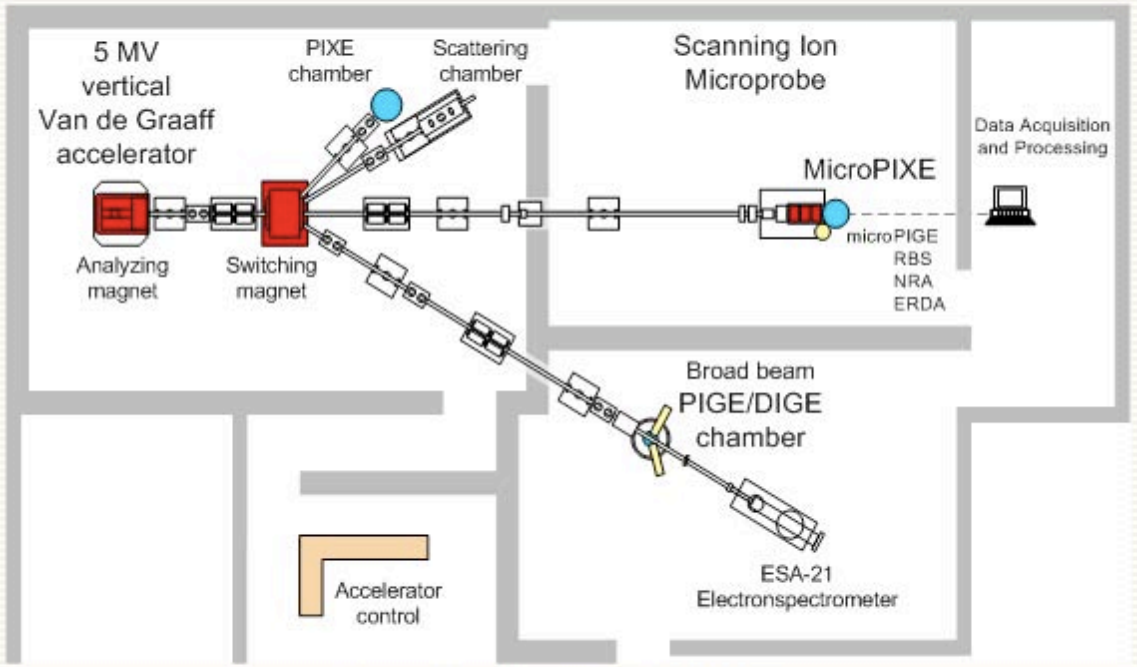

Schematic diagram of the IBA Lab.

http://iba.atomki.hu/facilities.html

Micro-PIXE analysis of an Egyptian Papyrus

Identification of the pigments used for the "Book of the Dead"

A-M. B. Olsson[1], T. Calligaro[2], S. Colinart[2] , J.C. Dran[2], N.E.G. Lövestam[3], B. Moignard[2] and J. Salomon[2]

[1]University of Göteborg, SE-405 30 Göteborg, Sweden

[2]Centre de recherche et de restauration des musées de France, CNRS UMR 171, Palais du Louvre Paris, France

[3]Chalmers University of Technology, SE-412 96 Göteborg, Sweden

http://www.fastcomtec.com/n-applications/multiparameter-systems/micro-pixe-analysis.html

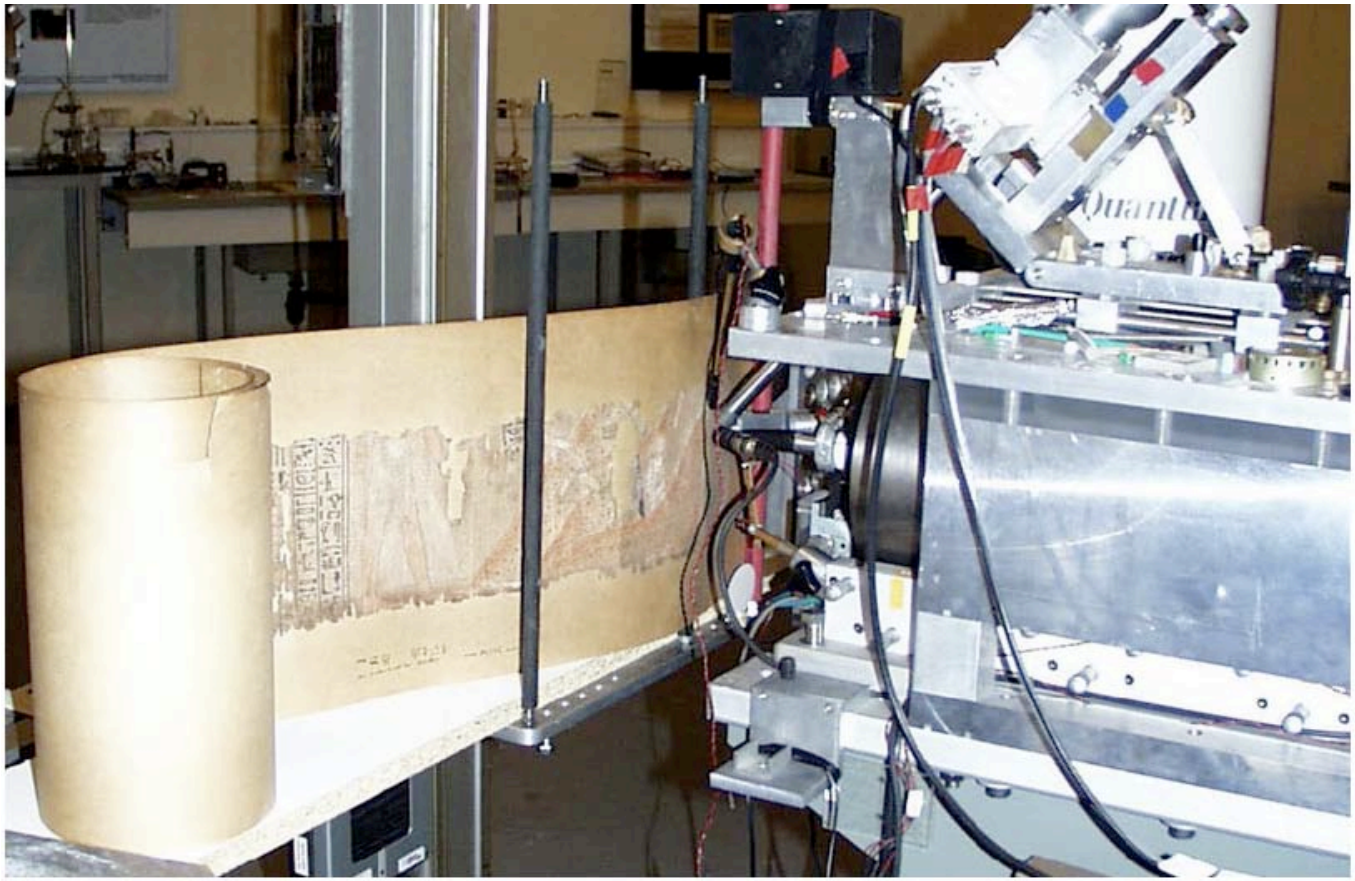

View of the external microprobe set-up with the papyrus in place

The Papyrus KM 21933 consists of hieroglyphic text ended by a painted vignette. It forms the right end of a "Book of the Dead" from the Theban 19th Dynasty (c.1295- 1186 B.C.). This name is given to religious funerary texts and spells for protection and guidance of the deceased entering the afterlife. Probably discovered in the 1820´s, it was acquired in Berlin in 1912 by The Kulturen Museum in Lund, Sweden.

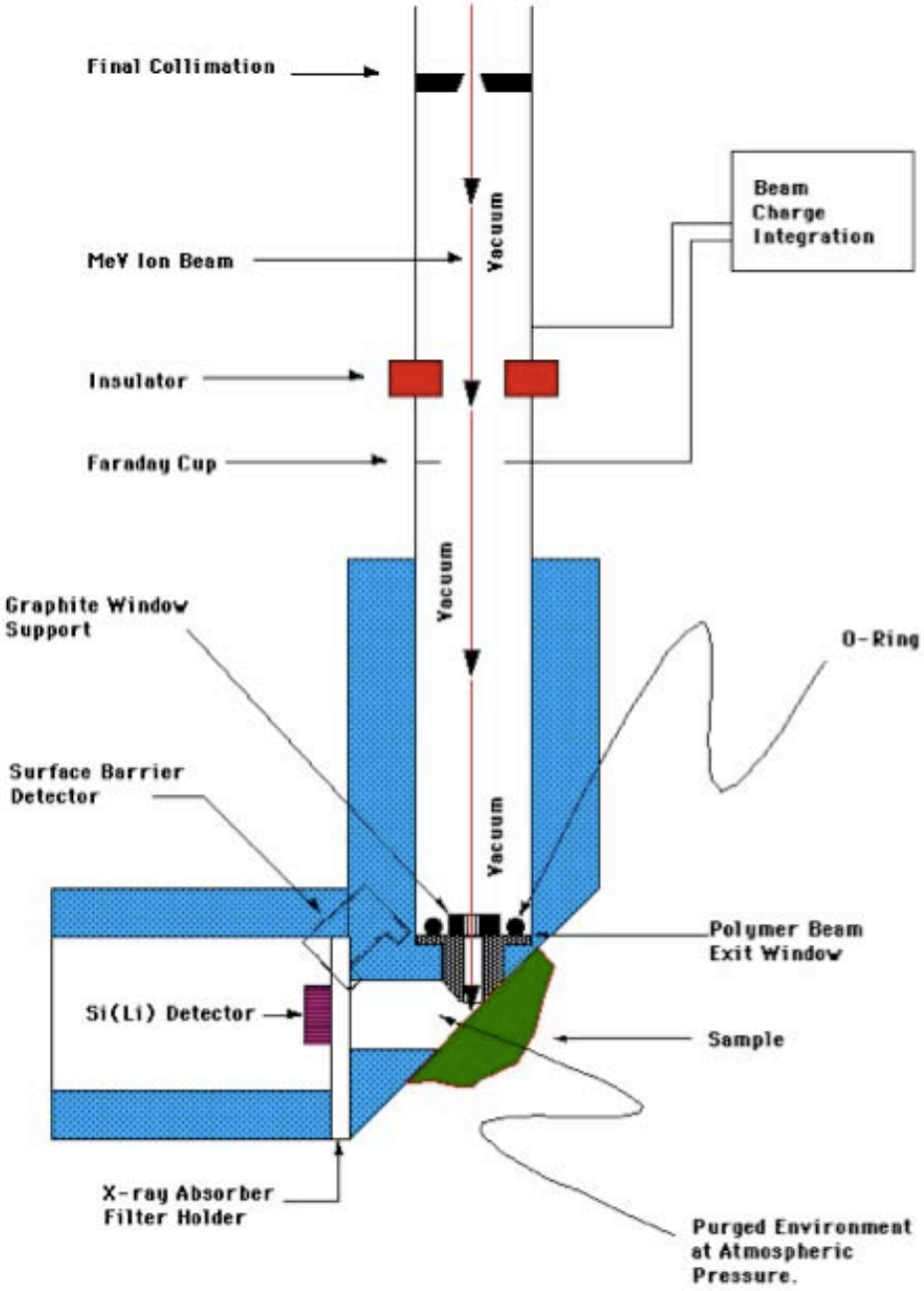

HARVARD PIXE SYSTEM

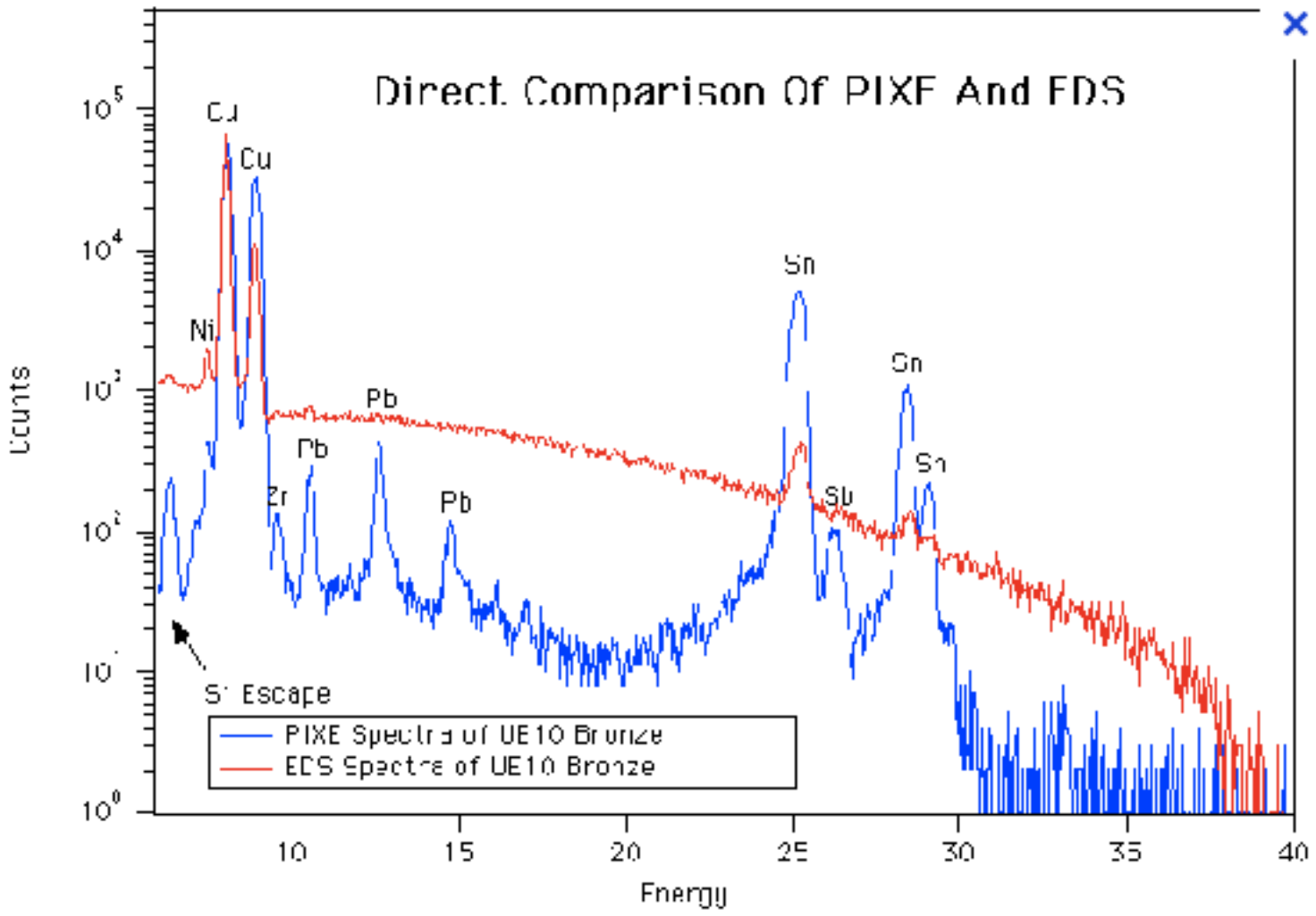

From http://www.mrsec.harvard.edu/cams/PIXE.html

Particle Accelerators in Art & Archaeology

Pier Andrea Mandò

Dipartimento di Fisica
and Sezione INFN, Florence, Italy

e-mail mando@fi.infn.it

www.presid.infn.it/er/er04fazio.ppt

Erice, April 17, 2004

External-beam PIXE analysis of the frontispiece of Pl.16,22, from Biblioteca Laurenziana in Florence

PIXE analysis of ancient manuscripts

(INFN Firenze, Biblioteca Vaticana, Biblioteca Laurenziana)

Detecting which pigments were employed provides important art-historical information, both about general trends and specifically about the analysed work.

More or less precious materials ↔ symbolic value of the text.
Trade routes of raw material import from countries far away. Added or restored parts.

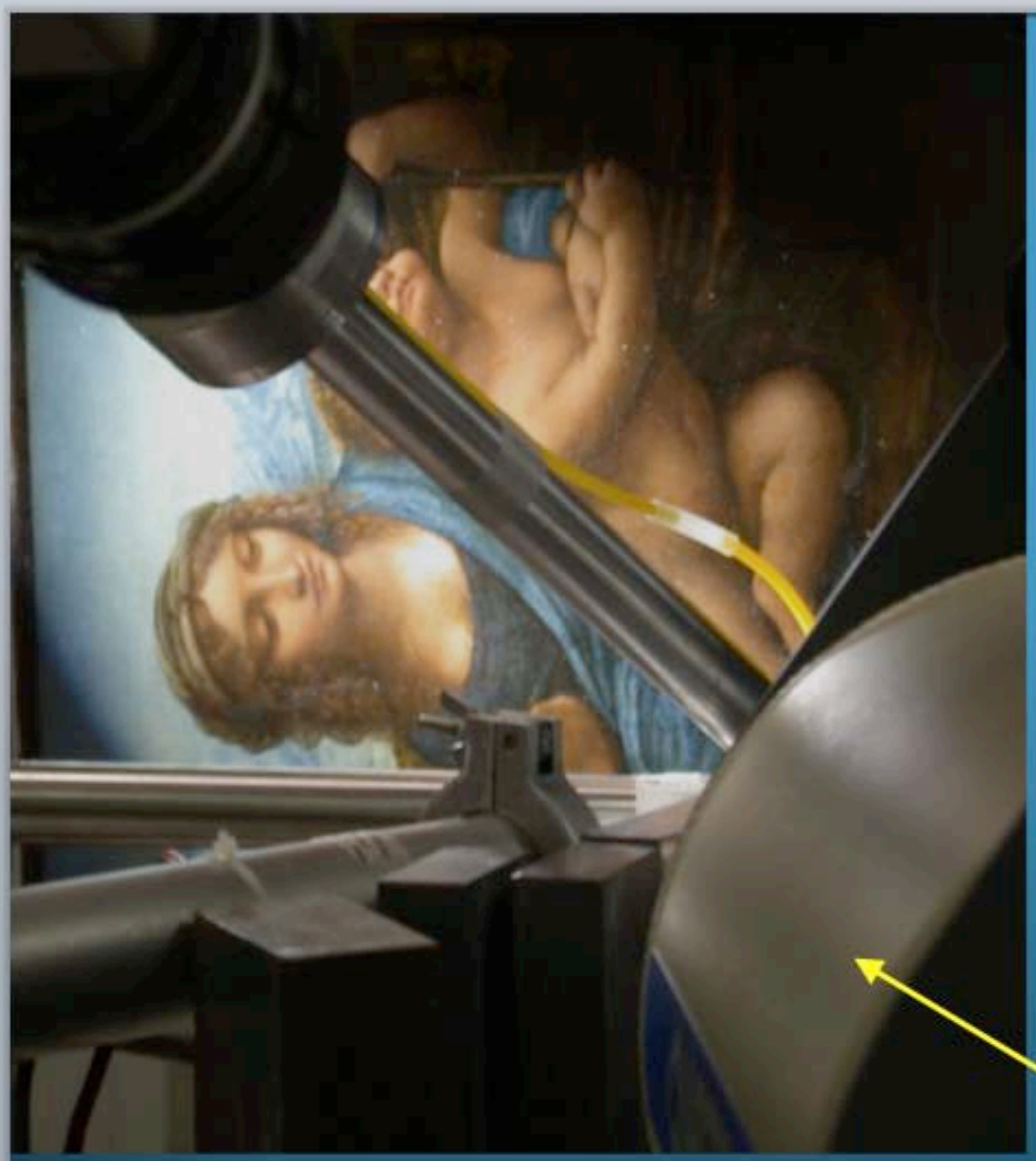

differential PIXE to discriminate the contributions of different layers

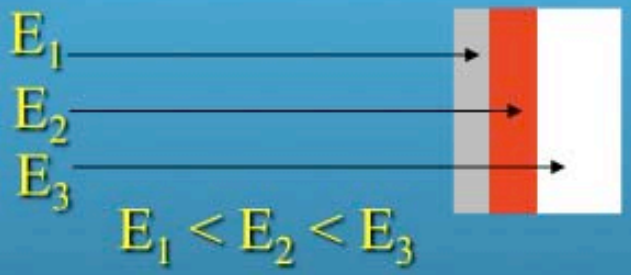

+ simultaneous use of PIGE to detect light elements

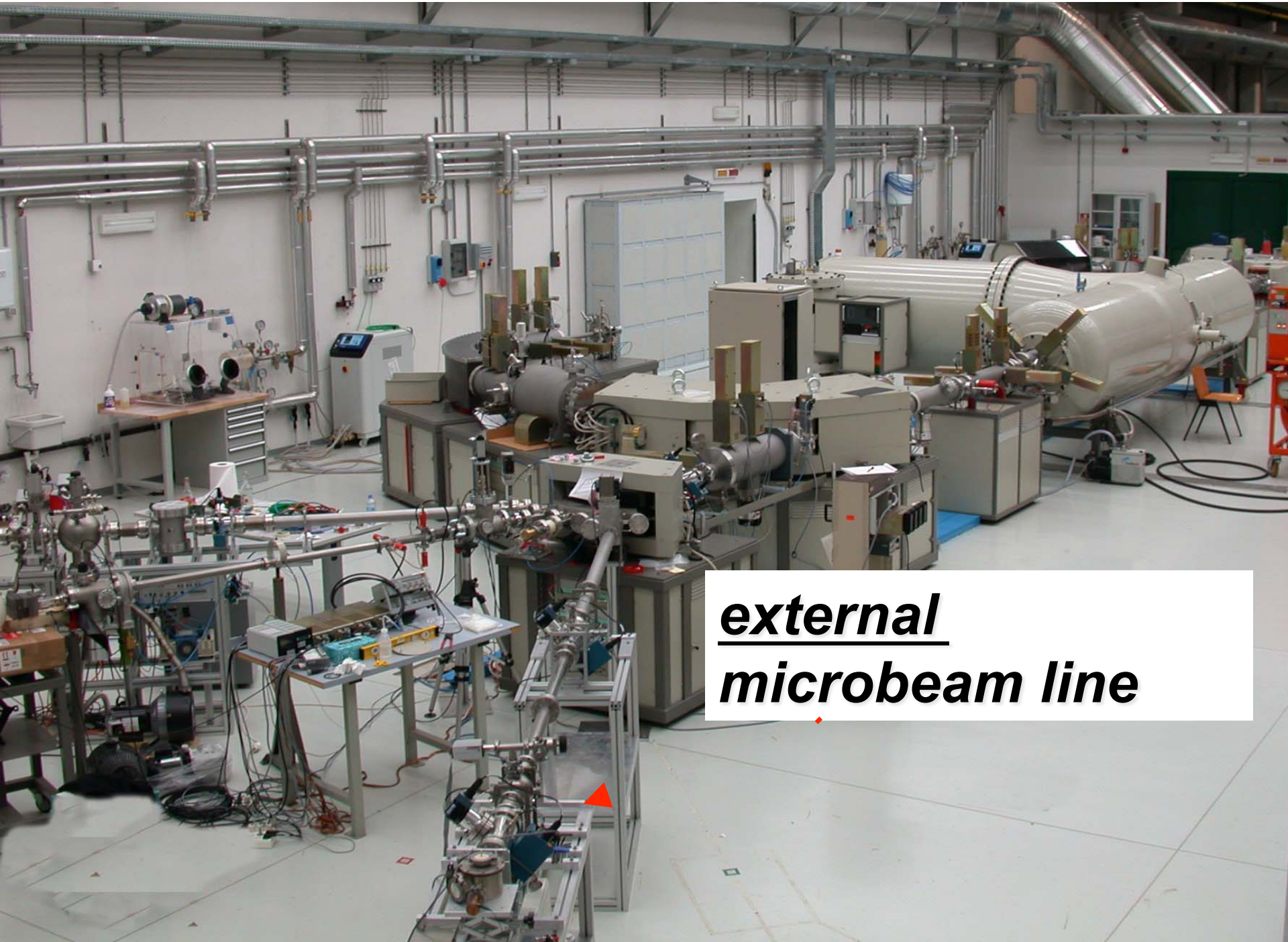
external
microbeam line

Final Paper/

1. Paper due last day class
   10 page approx.
   (IEEE style references)

2. Rough outline due February 26 or earlier

3. Topic should be about a particular microcharacterization technique and comparison with at least one other method. From topics covered in course outline.

4. You must discuss the spatial resolution characteristics and limits.

5. *Include the abstract of each paper you reference or a one paragraph summary of the url reference.*

6. Briefly, discuss a particular application.

EE213 Paper Notes

- See IEEE.jour for formatting notes. On class web site.
- Paper should be about 10 pages long including figures.
- Paper should include a 1 paragraph abstract
- Paper should have at least 10 references.
- For each reference, either a summary or the abstract of that reference attached as an Appendix to the paper.

Possible topics for paper

SEM imaging
Quantitation in the SEM
Auger microscopy/spectrosocpy
Particle beam induced Xray spectroscopy
(electrons, ions, photons, etc.)
Xray Microscopy
SIMS microscopy
RBS microanalysis
Super resolution optical microscopy
Scanned tip microscopy
Atom probe microscopy
Tomography
Other topics (upon approval)